Accepted Manuscript online: 2023-04-19 Article published online: 2023-05-16

Vapor-Deposited Polymer Films and Structure: Methods and Applications

Fang-Yu Chou[#,a]
Theresia Cecylia Ramli[#,a]
Chin-Yun Lee[a]
Shu-Man Hu[a]
Jane Christy[a]
Hsien-Yeh Chen[*,a,b]

[a] Department of Chemical Engineering, National Taiwan University, 10617 No. 1, Section 4, Roosevelt Road, Taipei City, Taiwan
[b] Molecular Imaging Center, National Taiwan University, 10617 No. 1, Section 4, Roosevelt Road, Taipei City, Taiwan
[#] These authors contributed equally to this work.
[*] hsychen@ntu.edu.tw

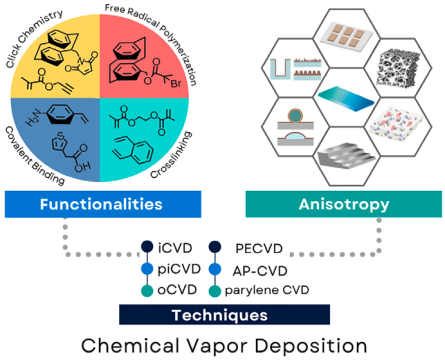

Received: 02.12.2022
Accepted after revision: 12.04.2023
DOI: 10.1055/a-2076-8570; Art ID: OM-2022-12-0051-SR

Abstract Vapor deposition of polymers is known to result in densified thin films, and recent developments have advanced these polymers with interesting fabrication techniques to a variety of controlled structures other than thin films. With the advantages of chemical modification and functionalization of these polymers, advancements have combined both the physical and chemical properties of these vapor-deposited polymers to obtain controlled anisotropic polymers, including layer-by-layer, gradient, hierarchical, porosity, and the combination of the above, meaning that the produced polymers are functional and are addressed in devised physical configurations and chemical compositions. The main purpose of using polymer coatings as a tool for surface modification is to provide additional properties that decouple the natural properties of the underlying materials (including metals, polymers, oxides/ceramics, glass, silicon, etc.), and recent advancements have rendered novel insights into combined physical and chemical properties to fulfill the increasing needs of sophisticated requirements of materials for users. The review herein intends to deliver messages of recent progress of the advancements of vapor-deposited polymers, with discussions of the variations of the physical structures and chemical functionalities, and how these two aspects are integrated with novel fabrication techniques. The advanced vapor polymers now have the capability of controlled anisotropy in the physical structure and chemical composition and are expected to pave the way for interface engineering toward prospective material designs.

Table of content:

Key words: vapor deposition, polymer coating, surface modification, surface structures, material interfaces

1. Introduction

Vapor deposition to prepare thin-film coatings renders attributes including a dry and clean process, excellent film quality and uniformity, and the deposition coating process is also reliable with high control and reproduction fidelity.[1] Vapor deposition processes are also widely implemented in current industrial production and in many discipline fields, e.g. semiconductors, electronics, biomedical devices, etc.[2] These vapor-deposited thin films are mostly inorganic materials such as metals, oxides, metal-organics, and/or their combination and derivatives and are in some minority cases polymer thin films; even fewer cases are industrialized into mass production (e.g. Parylene™). That is, the vapor deposition of polymeric thin films is still in the research development stage, and altering the interface properties of existing materials, including metals, polymers, oxides/ceramics, glass, and silicon, is widely discussed, using these vapor-deposited polymers as surface modification tools and achieving new properties that the original materials do not possess. This interface technology of polymer thin films shows promise in current materials science to provide controlled surface engineering properties and has successfully demonstrated new possibilities and applications for prospective materials with current existing materials.[3,4] With the same merits of the vapor deposition process (dry process and conformal film uniformity) described above, vapor-deposited polymers provide an additional variety of chemical functionalities, and post- and more sophisticated conjugation chemistry or multifunctionality[5,6] can be further executed.[7–14] Furthermore, from the physical prospective point of view, these vapor-deposited polymers are available for structuring/patterning with lithographic techniques and render confined compartments at the micro/nanoscale of these functional polymers.[15] These combined physical and chemical properties also lead to controlled anisotropy in which the layer-by-layer arrangement, gradient, hierarchy,

Biosketches

Fang-Yu Chou received her Ph.D. degree from the Department of Bioengineering at University of Tokyo (Japan) in 2021 and her M.E. degree from the Department of Chemical Engineering at the National Taiwan University. She is currently a postdoctoral research fellow working with Professor Hsien-Yeh Chen at National Taiwan University Department of Chemical Engineering. Between her last graduated school and a Ph.D. degree, she worked as a research assistant in the Genomics Research Center at Academia Sinica. Her research interests focus on interfaces for biomaterials and surface modification, tissue engineering, biomaterials science, and medical devices.

Theresia Cecylia Ramli received her bachelor's degree in Chemical Engineering from Bandung Institute of Technology (Indonesia) in 2017. She is currently pursuing her Ph.D. degree under the guidance of Professor Hsien-Yeh Chen at National Taiwan University. Her research mainly focuses on fabricating functional polymers by using chemical vapor deposition technology for biomedical applications.

Chin-Yun Lee received her B.S. degree from the Department of Chemical Engineering at National Taiwan University in 2020. She is currently a Ph.D. student under the guidance of Professor Hsien-Yeh Chen at National Taiwan University. Her main research interests include the synthesis of multifunctional polymers using chemical vapor deposition and surface modification to develop functional coatings for biomedical applications.

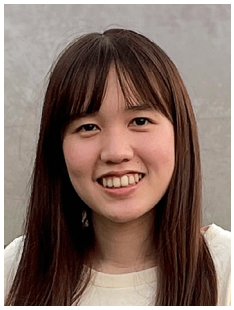

Shu-Man Hu received her B.S. degree from the Department of Chemical and Materials Engineering at National Central University in 2020. She is currently a Ph.D. candidate associate in the Department of Chemical Engineering at the National Taiwan University, under the guidance of Professor Hsien-Yeh Chen. Her research interest focuses on fabricating modular and multifunctional tissue engineering scaffolds using chemical vapor deposition technology.

Jane Christy received her B.S. degree in Chemical Engineering from National Taiwan University in 2022. She then remained to pursue her M.S. degree in the university and is currently a student in Prof. Hsien-Yeh Chen's research lab. Her current research interests include fabrication of tissue engineering scaffolds and surface modification of biomaterials with chemical vapor deposition.

Hsien-Yeh Chen is a full professor in the Department of Chemical Engineering and also the director of the Molecular Imaging Center at the National Taiwan University. He received his M.Sc. and Ph.D. degrees from the University of Michigan (U.S.A.) in 2004 and 2008, respectively. He carried out his postdoctoral research in the Karlsruhe Institute of Technology (KIT) in Germany. His research interests focus on biomaterials interfaces and the fabrication processes, biomolecular engineering, nanoparticle technology, implantable medical devices, and chemical vapor deposition (CVD) polymerization, for biotechnological applications.

and compartmentalization of the devised properties can be addressed, as well as organizing the materials into selected configurations from 2D to 3D.[16] Applications of using these vapor-deposited polymers from thin films to structural devices have shown promising results and have delivered novel concepts for prospective material design in many materials science disciplines.

In this review, we highlight the developments in vapor deposition of polymers with the possibility of a variety of physical structures, including thin films, patterned structures, and even 3D and porous structures. From both physical and chemical perspectives, the production and use of these vapor-deposited polymers are discussed. The advanced fashion of producing these polymers into controlled gradient, compartmentalized, and hierarchical distributions is also shown with interesting fabrication processes. Finally, some important applications of using these polymers are demonstrated with some featured examples. Although not comprehensive, the review herein is intended to deliver insight into vapor-deposited polymer technologies with their current advances, and we expect that there will be more novelty and concepts to overcome current challenges and to fulfill the increasing needs of prospective materials and interfaces.

2. Fabrication and Materials

Polymer thin films are a growing field due to their versatility and immense technological potential in functionalizing materials and devices. They exhibit many different functions, including tailoring the surface energy, enhancing adhesion, providing insulation, acting as organic barriers, and providing stimuli responsiveness, UV protection and many other additional properties.[17] These functions make polymer thin films applicable for many fields, including biomedicine, sensors, microelectronics, and optics. Currently, the research trend in polymers has started to shift from 2D substrates to the fabrication of free-standing nanomaterials such as nanoparticles, nanotubes, and nanowires.[18] Polymer nanostructures possess advantages over other types of nanomaterials, as they are easily tunable, their structures can be altered to produce structures with various compositions, morphologies, sizes, and surface properties.[19] Vapor deposition has emerged as a promising technology for polymer synthesis because of its unique properties over traditional solvent polymerization. Vapor deposition enables (1) solvent-free, uniform and conformal large-area film fabrication on both planar surfaces and 3D geometries[20] and (2) real-time control over the thickness and nanostructure of growing films.[21] Vapor deposition is a technique in which the coating ingredient evaporates into atoms, molecules, or ions and then condenses onto the substrate surface.[22] Chemical vapor deposition (CVD) and physical vapor deposition (PVD) are two types of vapor deposition techniques. Vapor deposition is especially suited for synthesizing insoluble or infusible polymer thin films such as fluoropolymers, crosslinked organic materials, and conjugated polymers.[23] Rather than utilizing atoms as film-building species like in PVD methods, e.g. sputtering or evaporation, reactive molecules or radicals in CVD construct a polymeric film through a chemical reaction.[24] CVD polymerization includes a wide range of deposition processes, such as initiated CVD (iCVD), oxidative CVD (oCVD), plasma-enhanced CVD (PECVD), photoninitiated CVD (piCVD), and atomic layer deposition. The CVD variations most commonly utilized to fabricate polymer thin films are iCVD, piCVD, PECVD, oCVD and parylene CVD, which will be the emphasis of this section. The comparisons of these techniques are listed in Table 1. The following section will discuss the CVD techniques used to fabricate polymer thin films and structures, as well as the material physical attributes and functionality that each process produces.

2.1 Processing Technologies

CVD systems are fundamentally composed of three elementary stages. First, the reactant gases are delivered into the deposition chamber through the gas inlet. Second, in the deposition chamber, the precursors undergo gas-phase reactions to activate them and enable subsequent polymerization on the substrate surface. Heterogeneous reactions at the gas–solid interface led to continuous thin film development. Finally, gaseous products and unreacted species are removed through the gas exhaust.[25,26] CVD methods are fre-

Table 1 Comparisons of several polymer thin-film fabrication methods

Method	Polymers	Initiators	Common substrates	Mechanism	Advantages	Film features	Ref.
iCVD	**Monovinyl** PHEMA, PHEMAx, and PGMA **Multivinyl** PMAH, PDVB, PV3D3, and PHPFO	*tert*-butyl peroxide (TBPO) Perfluorobutanesulfonyl fluoride (PFBSF)	Silicon wafer Glass Mesoporous TiO_2	Chain-growth polymerization	Wide variety of monomers One-step copolymerization of composite film Functional retention of the deposited polymer	Hydrophobic/hydrophilic properties Stimuli-responsiveness (thermal and pH) Mechanical robustness Gradient properties	31,37–70
piCVD	Photoinitiative monomers, e.g. PHEMA, PHEMAxE, GDA, PHEA, and PTFOA	Photoinitiator: ultraviolet (UV) light	Silicon wafer Sodium-sensing optode Polymers (as wearable sensors)	Chain-growth polymerization	High crosslinking High deposition rate control Operable at atmospheric pressure and room temperature	Biocompatible Enhanced cell adhesion Mechanical robustness Hydrophobic/hydrophilic properties	35,71,72
PECVD	Graphene Carbon nanotubes	Cold plasma Gas: O_2, CF_4, and Ar	Silicon wafer Stainless steel SiO_2, Al_2O_3, Ni Cu foils PDMS	Chain-growth polymerization	High deposition rates Wide variety of monomers	Thermal-responsiveness Hydrophobic/hydrophilic properties	36,73
AP-PECVD	PNVCL PV4D4	Dielectric barrier discharge (DBD) plasma Gas: Ar and O_2	Silicon wafer PDMS	Chain-growth polymerization	Operable at atmospheric pressure	Antimicrobial properties Insulating properties	74,75
oCVD	PEDOT Polypyrrole (PPy)	Gas oxidants: metal halogen salt or halogen gas, e.g. $Fe(III)Cl_3$ and $CuCl_2$ Liquid oxidants: antimony pentachloride ($SbCl_5$); vanadium oxytrichloride ($VOCl_3$)	Silicon wafer Fiber Glass Polycrystalline ZnO	Step-growth polymerization	High conformity	Mechanical robustness Enhanced adhesion Patterned film Electrical conductivity	76–85
Parylene CVD	Parylene N Parylene C Parylene AF4 Parylene D Parylene HT Parylene F	–	Silicon wafer Glass PDMS	–	Wide variety of functional groups Facilitation of chemical conjugations	Antifouling properties Antimicrobial properties Anticorrosion properties Hydrophobicity Thermal stability	18,86–105

quently named after their energy sources, such as PECVD, or reaction mechanisms, such as iCVD or piCVD.[26]

The iCVD uses free-radical volatile initiators, such as *tert*-butyl peroxide (TBPO), and precursors containing vinyl bonds for the polymerization process. Polymer synthesis and film manufacturing may be accomplished in a single step by using this method.[2,27] The iCVD approach mimics chain-growth synthesis in solvent polymerization to produce electrically insulating polymers with desired organic functional groups. Some of the merits of iCVD include conformal surface modifications, precise control of polymer chemistry, a vast library of functional groups, minimal by-product formation, and compatibility with delicate substrates, making it suitable for a wide range of applications.[2,26,28] Welchert et al. used an oblique angle to introduce monomer vapor to the substrate to pattern *n*-butyl acrylate (nBA), methacrylic acid (MAA), and 2-hydroxyethyl methacrylate (HEMA) polymer films during iCVD.[29] A uniform coating can also be enhanced by utilizing a speaker to vibrate the substrate.[30] Chen et al. demonstrated that iCVD is a useful technique for creating well-integrated polymer–nanostructure systems that can be used to study how polymers behave in nanoconfined environments.[31] In another study, Mao et al. demonstrated the versatile application of iCVD by showing the use of iCVD to stabilize an electrochemically active polymer, polyvinylferrocene, by soft confining it with P(2-hydroxyethyl methacrylate-co-di(ethylene glycol) divinyl ether) (P(HEMA-co-DEGDVE)) using the iCVD method.[32] Monomers that were used in the iCVD method have been tabulated and can be seen in the review by Gleason.[33]

A variant of iCVD known as piCVD uses UV light rather than thermal light to activate the initiators. This enables the activation of certain methacrylate monomers without the need for thermally labile and short-lived initiators used

in iCVD.[26,34] The use of photoinitiators also eliminates the use of high-temperature sources. However, this method has a drawback in that the reactive mixture must be photosensitive, and as such, only a certain number of monomers can be used. This limitation, on the other hand, aids in reaction control by allowing the molecules on the substrate to restructure. As a result, piCVD produces more crosslinked structures.[35]

A CVD process that is similar to piCVD is PECVD; instead of using UV light, PECVD uses cold plasma to initiate free-radical polymerization. The use of plasma enhances the PECVD versatility due to its high energy transfer to the reactive species. For example, PECVD enables the deposition of inorganic–organic composite films in one chamber.[36]

PECVD has been used to functionalize nanoparticles and fabricate carbon nanotubes.[35] The issue with this technique is that it often leads to unstructured coatings. This is because the release of a wide range of species causes nonspecific reactions to occur.[34,35] Pulsed-PECVD, one of the variants of this technique, uses pulsed plasma to allow the restructuring of the coating. To eliminate the use of vacuum pressure, which is required by the PECVD technique, PECVD has been improved to be capable of working at atmospheric pressure, making scaling up easier; this process is known as atmospheric pressure plasma-initiated CVD (AP-piCVD). This method uses temporally isolated discharge to initiate the polymerization. By using this method, Loyer et al. successfully copolymerized *N*-vinyl caprolactam (NVCL) with ethylene glycol dimethacrylate (EGDMA) to fabricate water-soluble and water-stable thermoresponsive thin films.[34] Getnet et al. (2020) also used this method to deposit carvacrol extract on stainless steel to prevent the formation of biofilms.[74] The resulting films adhere well to the substrate and remain stable for a long time when exposed to UV light and air. Coclite et al. used initiated plasma-enhanced CVD (iPECVD) of an organosilicon polymer (1,3,5-trivinyl-1,1,3,5,5-pentamethyltrisiloxane [TVTSO] monomer) to planarize silicon substrates and demonstrated that when the organic thin film is 1.8 nm thick, a 99% degree of global planarization could be achieved.[107] For graphene film growth by atmospheric pressure CVD on copper foil, the final graphene film's homogeneity and electronic transport properties were found to be strongly influenced by the surface morphology of the Cu substrate and the concentration of carbon feedstock gas, as reported by Luo et al.[109]

Another type of CVD used to fabricate thin films is oCVD. Unlike iCVD that employs chain-growth polymerization, oCVD implements step-growth polymerization. Rather than using an initiator, oCVD uses an oxidizing agent, such as an evaporated metal halogen salt, or halogen gas, such as vapor iron(III) chloride. Together with the vaporized monomer, for example, 3,4-ethylene dioxythiophene (EDOT), it is injected into a vacuum chamber with a hot wall to begin polymerization.[110] The oCVD method allows for the development of grafted interfaces for firmly adherent layers. Additionally, oCVD enables conformal coverage where layers with the same thickness can be deposited over nonplanar structures, such as rough surfaces. Vapor printing or patterning films could also be fabricated by using this method.[23] The oCVD is preferred for fabricating electrically conducting or semiconducting films since it offers control over the morphology of the conjugated polymers, which leads to optimization of their optoelectronic characteristics.[27] For example, simply by adjusting the substrate's temperature, it is possible to modify the polymer electrical conductivity.[111] As shown by Wang et al. (2018), by inducing a crystallite-configuration transition by oCVD and heating the substrate to 300 °C, poly (3,4-ethylenedioxythiophene) (PEDOT) thin films with a record-high electrical conductivity of 6259 S/cm and a remarkably high carrier mobility of 18.45 $cm^2 \cdot V^{-1} \cdot s^{-1}$ can be produced.[112] In addition to gaseous oxidants, liquid oxidants such as antimony pentachloride ($SbCl_5$) and vanadium oxytrichloride ($VOCl_3$) have also been used in oCVD to fabricate PEDOT thin films with conductivities exceeding 2100 S/cm, as shown by Kaviani et al. (2019).[113] They also demonstrated that one of the most important factors that affect the properties of the deposited material is the choice of oxidant. To date, the oCVD method has been used to fabricate organic conducting and semiconducting polymers that are being used in photovoltaic cells and biosensors.[23]

Parylene CVD is another type of CVD used in the fabrication of thin films. This CVD method, as the name implies, polymerizes [2.2]paracyclophanes (PCPs) to poly(*para*-xylylene) (PPX) or parylene. Following the Gorham process, PCP is sublimated to form its radical species, *para*-xylylene (*p*-xylylene), which spontaneously deposits on target surfaces that are typically kept at or below room temperature.[114] Parylene could be deposited as thin, conformal, pinhole-free films using CVD, with the thickness adjustable by changing the amount of precursor used for CVD polymerization.[115] Patterned coatings can also be achieved by using CVD, and patterning can occur after the CVD process or during the CVD process.[116] By using this technique, a variety of functional groups can be added to parylene, allowing its surface chemistry to be further modified for various applications.[26] Parylene, especially parylene C (mono-chloro-PCP), is known for its high biocompatibility, anticorrosive properties, and antibacterial properties, making it suitable as a biomaterial.[18] Other parylenes that have been fabricated with CVD include parylene N (nonfunctionalized), parylene D (di-chloro-PCP), and parylene-HT (tetra-fluoro-PCP). Tian et al. deposited parylene AF4 (octafluoro-[2.2]paracyclophane) onto polydimethylsiloxan (PDMS) to create a surface with wrinkled surface topography, low surface free energy, and negative surface charge properties that exhibited antifouling performance against bacteria and algae.[86] A variety of functionalized groups used in parylene CVD have been fully reviewed by Hassan et al.[18] Sim et al. developed a sin-

gle-step bifacial vertical deposition method to address the issue of thickness variations on both sides of the sample that arise during traditional horizontal deposition.[106] In another study, Hu et al. used a sublimating ice template as the CVD substrate to produce an advanced functional porous material that is capable of conjugating with thiol-Michael click chemistry.[93] Protocols to examine and characterize PPX layer stability properties, including thermostability and adhesive strength, and biocompatibility (cell viability and immunological responses) were proposed by Hsu et al.[117]

2.2 Physical Properties

Thin films made by vapor deposition have a wide range of properties that are dependent on the process, monomers, and substrates used to fabricate them. The control of film properties could be achieved by fine-tuning the system parameters such as monomer flow rates, plasma power or filament temperatures.[38] This section will discuss the physical properties of vapor-deposited fabricated films, such as thickness, morphology, mechanical properties, and electrical conductivity, and factors that affect them. The physical properties discussed in this section are shown in Figure 1.

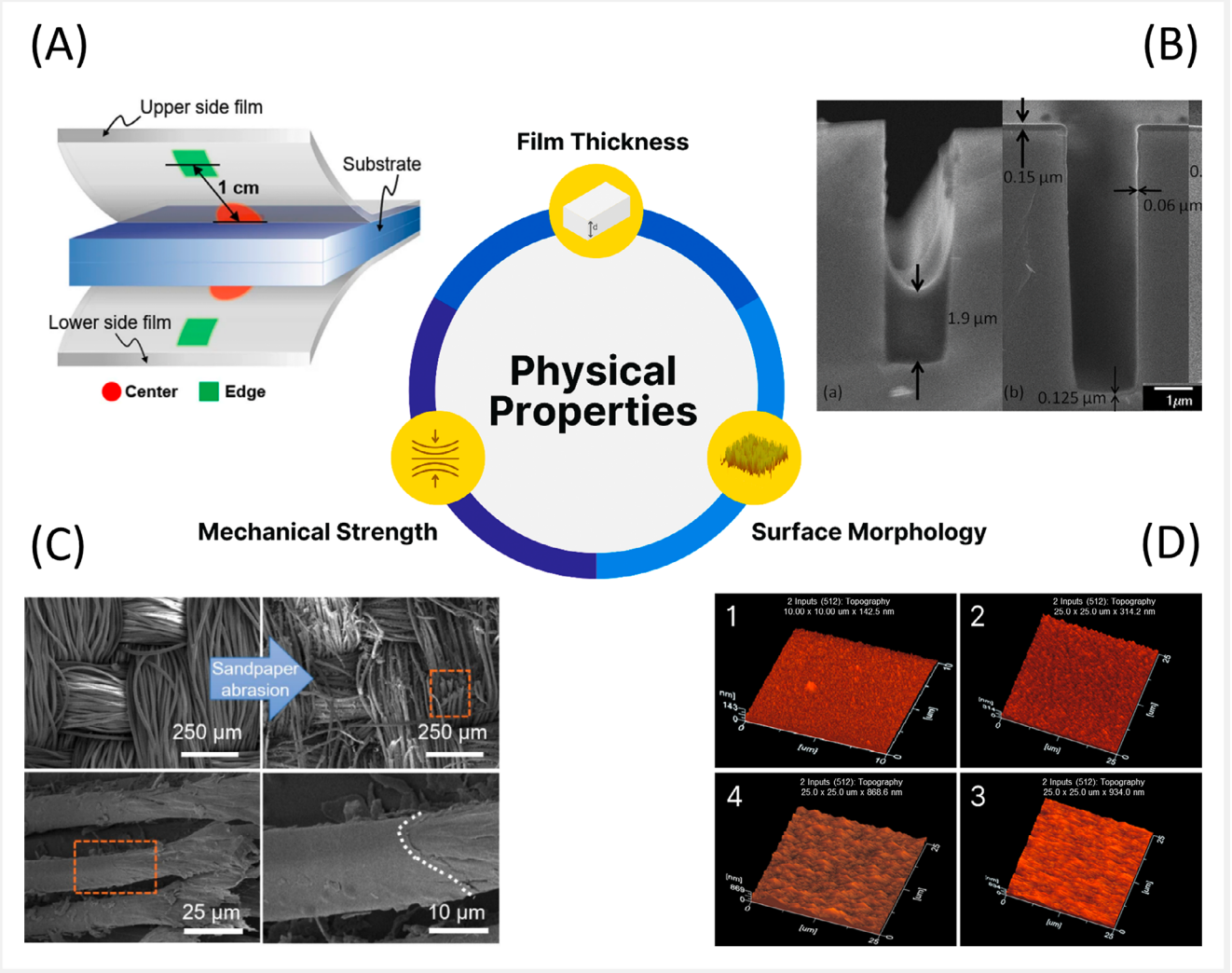

Figure 1 Schematic diagram of the fundamental physical properties of thin films. (A) Schematic diagram of the two-sided deposition of parylene C onto a silicon wafer substrate with vertical deposition.[106] Reprinted from Ref. 106 published under a creative commons license (CC BY). (B) Cross-sectional scanning electron microscopy (SEM) images of iPECVD-grown PTVTSO on a trench wafer substrate.[107] Reprinted with permission from Ref. 107. Copyright 2012 AIP Publishing. (C) SEM images of p(C6-co-IEM)-coated PET fabric before (upper left) and after 1,000 cycles of sandpaper abrasion (upper right), as well as close-up views of the coatings after 1,000 cycles of sandpaper abrasion (bottom).[108] Reprinted with permission from Ref. 108. Copyright 2020 Elsevier. (D) AFM measurements of surfaces with smooth and rough characteristics for parylene N (no. 1, 4) and parylene C (no. 2, 3) deposited with PECVD (top) and CVD (bottom).[73] Reprinted from Ref. 73 published under a creative commons license (CC BY).

Montero et al. used piCVD to copolymerize HEMA and the functional comonomer pentafluorophenylmethacrylate (PFM) and discovered that varying the precursor flow rates during deposition enables the fabrication of films with thickness gradients.[118] This is consistent with the findings of Welchert et al., who used oblique angle iCVD to polymerize n-nBA, MAA, and HEMA on silicon wafers and discovered that the flow rate of the monomer is the major parameter that affects the thickness profile.[29] In another study, Sim et al. used vertical deposition of parylene to fabricate a parylene C thin film on both sites of the substrate simultaneously with the same and uniform thickness.[106] Profiling thin films is also important to achieve an understanding of the thin film characteristics. Chen et al. developed an experimental method that combines ion milling and high-resolution field emission scanning electron microscopy to acquire a precise and accurate depth profile of the coating thickness and iCVD kinetics along nanopores with a diameter of 110 nm.[119] For copolymerization of hybrid organic–inorganic polymeric films, uniform thickness could be achieved by using modified iCVD with a dual showerhead injector, as shown by Kim et al.[120]

Surface morphology or roughness is another parameter that depends strongly on the CVD method and is usually characterized with atomic force microscopy (AFM). As compared by Gerhard, parylene C fabricated by PECVD shows smoothness compared to that fabricated by CVD. Surface roughness is one of the major causes, in addition to the existence of hydrophilic functional groups, that could influence the hydrophobicity of thin films.[73] Smoothening the surface can enhance its wettability. To achieve this, the deposition rate must be kept low to direct the polymerization toward surface polymerization rather than volume polymerization and produce a higher film quality.[121] As shown by Chen et al., treating parylene CVD with plasma CF_4 could trigger volume polymerization, which will produce roughened surfaces with low hydrophilicity.[73,122] Therefore, the hydrophilicity of parylene films is tunable with plasma treatment either temporarily or permanently, and superhydrophobic surfaces can be fabricated at a minimal cost. Gołda et al. reported that by using oxygen plasma to fabricate nanoroughness on a parylene surface after the CVD process, the contact angle could be decreased, thereby increasing the hydrophilicity.[123] Brancato et al. also concluded that by strategically adjusting the plasma exposure times, the degree of hydrophobicity of the prepared surface can be precisely controlled.[124] Surface roughness also plays an important role in the adhesion of parylene coating to silicon wafers or metals, and adhesion can be increased by enlarging the surface/volume ratio.[122] In a different study, Hsu et al. discovered that with parylene CVD, a slightly rougher surface will be produced at a higher sublimation rate.[125] The increase in roughness is due to the higher deposition pressure. Therefore, increasing the sublimation rate to increase film thickness or production throughput should be done with surface roughness in mind. However, with oCVD and vapor phase polymerization (VPP), which use oxidants, it has been reported that rapid polymerization resulting from high redox activities increases the film roughness.[126] To counter this problem, Goktas et al. demonstrated that the addition of water vapor while fabricating PEDOT thin films results in better molecular alignment for oCVD PEDOT and a smoother surface for VPP PEDOT.[127] Additionally, they discovered that during the VPP process, temperature and water vapor both affect the surface roughness. Besides the deposition rate, the surface roughness also depends on the CVD substrate, as investigated by Amirzada et al.[128] As with oCVD, the PEDOT thin-film crystallographic texture can vary depending on grafting, control of the growth temperature and film thickness and the choice of oxidant.[28] PEDOT produced with oCVD has an edge-on orientation, in contrast to PEDOT prepared by liquid oxidants, which has a face-on orientation.[129] Moni et al. reported that edge-on thin films provide higher specific capacities for a given charge/discharge rate and therefore display electrochemical activity.[130]

Mechanical properties are the physical properties a material shows when subjected to forces and include the modulus of elasticity, tensile strength, elongation, hardness, and others. Zhao et al. showed that the mechanical properties of poly(divinylbenzene) (PDVB) films fabricated by iCVD on silicon wafers could be increased by incorporating a post-CVD thermal annealing process.[131] By using iCVD to fabricate self-crosslinkable poly(perfluorohexylethyl acrylate-co-isocyanato ethyl methacrylate), Shao et al. showed that the crosslinked network greatly improved the mechanical strength. Additionally, by enhancing the mechanical strength, the thin films are able to withstand a variety of durability tests, such as boiling for more than 12 hours and 20,000 cm of sandpaper abrasion.[108] This is consistent with the results of Lee et al. using iCVD to conjugate poly (2,4,6,8-tetramethyl-2,4,6,8-tetravinylcyclotetrasiloxane) (PV4D4) with PPFDMA, producing a PV4D4-PFDMA film with exceptional stability and durability due to crosslinking.[132] The tests showed better tensile strength and rubbing resistance compared to those of other films. Mechanical robustness was also shown to be enhanced by copolymerizing 2-hydroxyethylacrylate with glycidyl methacrylate (GMA) with the iCVD method in a study performed by Jeong et al.[133] This is because GMA contains a rigid methacrylate group.

Electrical conductivity is a major focus for PEDOT films synthesized using the oCVD method. Maintaining monomer fidelity in the film is crucial for producing high-conductivity conjugated polymers.[28] oCVD provides control over crystallite sizes and therefore control over electrical conductivity. Wang et al. used oCVD and demonstrated that by inducing a crystallite-configuration transition, PEDOT thin films with a record-high electrical conductivity of 6259 S/cm and a re-

markably high carrier mobility of 18.45 $cm^2 \cdot V^{-1} \cdot s^{-1}$ could be achieved.[112] Smith et al. found that the electrical conductivity, which ranges from 1 to 30 S/cm, does not clearly affect the thermal conductivity of oCVD-grown PEDOT films. It is believed that at these electrical conductivities, phonon transport predominates, and the electronic contribution to thermal conductivity is very small.[134] Therefore, CVD polymerization appears to be an appealing method for creating polymer films with low thermal conductivity and relatively high electrical conductivity values. Drewelow et al. proposed the conductivity in PEDOT films as a function of substrate temperature and thickness due to the enhanced crystalline and chemical environmental structures in PEDOT grown at higher substrate temperatures.[111] The conductivity increases with increasing substrate temperature initially and then decreases with increasing film thickness.

2.3 Chemical Functionality

The functionalities of thin films greatly depend on the functional groups of the monomers. These functional groups could enable covalent binding, surface chemistry such as alkyne–azide "click" chemistry, reactions of active esters with amine, aldehydes/ketones with hydrazides and alkoxyamines, and thiols with alkenes and alkynes and surface-initiated atom transfer radical polymerization (SI-ATRP)[135] to bring specific functions such as anticorrosion and enhanced biocompatibility, resulting in a multifunctional surface. Figure 2 summarizes the functionalized thin-film monomers discussed in this section.

CVD-grown parylene has especially demonstrated surface chemistry functionalities. For instance, Sun et al. used CVD to fabricate thiol-reactive parylene (poly(4-vinyl-*p*-xylylene)-co(-*p*-xylylene) and poly(4-*N*-maleimidomethyl-*p*-xylylene)-co-(*p*-xylylene). These functional groups enable thiol-ene and thiol-ene maleimide click reactions, respectively. The resulting surfaces suppress protein fouling and enhance surface affinity toward cell attachment.[136] Chen et al., in another study, also demonstrated the fabrication of alkyne-functionalized parylene on which poly(sulfobetaine methacrylate-co-Az) could be conjugated via click chemistry.[137] The conjugated polymers were remarkably stable and successfully reduced protein adsorption and cell adhesion. The findings show that the CVD technique offers a straightforward and reliable tool for producing antifouling surfaces on a variety of substrates. In another study reported by Im et al., iCVD was used to fabricate click-active surfaces via CuAAC chemistry by polymerizing poly(propargyl methacrylate) (PPMA).[138] In addition to the click reaction, CVD of parylene also shows its applicability in surface modification via atom transfer radical polymerization (ATRP). As reported by Jiang et al., CVD of [2.2]paracyclophane-4-methyl 2-bromoisobutyrate onto heterogeneous groups of substrates,

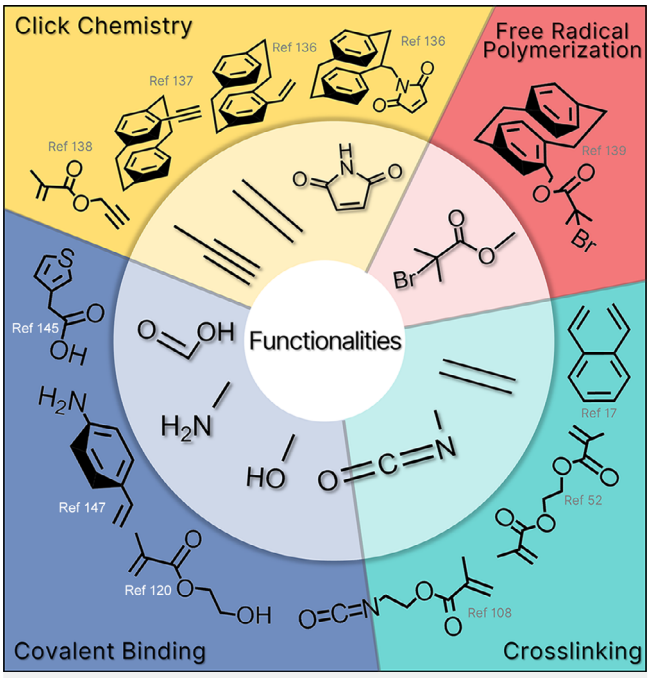

Figure 2 Schematic diagram of several functional groups of CVD monomers and their chemical functionalities.

such as silicon and glass, enables SI-ATRP, as confirmed by ATRP of oligo(ethylene glycol) methyl ether methacrylate.[139]

CVD also enables "covalent grafting" or covalent binding of polymers to substrates. Covalent binding promotes better adhesion of the thin film to its substrate.[140] As shown by Shao et al., copolymerization of a short-fluorinated side chain monomer, perfluorohexylethyl acrylate (C6), and isocyanato ethyl methacrylate (IEM) with iCVD to fiber as a substrate facilitated covalent binding with functional groups, such as hydroxyl, amino, and carboxylic groups, in the substrate, thus exhibiting excellent adhesion.[108] Covalent bonding also shows its functionality in patterning thin films. Patterns can be used to resist an underlying layer being patterned or to retain specific molecules or nanoparticles in place.[140] In another study, Vaddiraju et al. demonstrated that copolymerization of pyrrole with thiophene-3-acetic acid with oCVD enables covalent binding of thin films with metal nanoparticles.[145] This discovery opens the path for the development of conducting polymer–metal nanoparticle hybrids. Organic–inorganic binding is also enabled by –OH groups in the organic monomers that react with the inorganic precursors to form metal-oxide units in the polymer, as shown by Kim et al., who polymerized HEMA with inorganic precursors such as trimethyl alumina (TMA), tetrakis dimethyl amino hafnium (TDMAHf), tetrakis dimethyl zirconium (TDMAZr), and tetrakis dimethyl amino titanium TDMATi via iCVD.[120]

Crosslinking bonds have shown their importance in fabricating polymer thin films with high mechanical strength and hydrophobicity. Gao et al. demonstrated the feasibility of creating a thin film that is insoluble in a number of solvents and offers stainless steel corrosion resistance in concentrated 1 N HCl solutions by fabricating crosslinking PDVB via cationic CVD.[17] Shao et al., as mentioned above, polymerized highly reactive isocyanate groups that enabled self-crosslinking.[108] The fluorinated chains were fixed on the surface by crosslinking, which reduced the contact angle hysteresis causing the thin-film superhydrophobicity property. In another study, Soto et al. crosslinked 1H,1H-perfluorooctyl methacrylate (H_1F_7Ma) with DVB using iCVD and achieved an optimal combination between surface energy, permitted carbon chain length, and polymer chain rigidity, resulting in superior nonwetting fabrics.[146] On the other hand, in a study by Xu et al., covalent binding facilitated by the amine functional group in poly(4-aminostyrene) opens the opportunities for detection of various biomolecules.[147]

3. Controls of Anisotropy

Polymeric materials have been utilized in various applications. Depending on their applications, the chemical and physical properties of the materials are crucial. The monomer can change the bulk material properties for polymerization, processing parameters, or conjugating density. As we pointed out in section 2, materials with diverse chemical properties could be obtained by polymerizing functionalized monomers or utilizing functionalization on the surface. The material's structure, surface morphology, and anisotropic property are designed by changing the processing parameters. Recently, the requirement for anisotropic materials has increased with the development of various applications, such as permeation, medical devices, and tissue engineering. For example, an asymmetric porous membrane was fabricated into hollow fibers in an extracorporeal membrane oxygenation system.[148] In this section, fabrication techniques for preparing a membrane with a porous structure and nanotopographic surface that has become more critical will be discussed. We will focus on process design and combination with other techniques for the fabricated anisotropic membrane as technology requirements increase, along with the demand for multiple properties in materials. Thus, there has been a surge in research on compartment and composite materials. For example, organic–inorganic composite polymers showed better performance as electrolyte membranes.[149] At the end of this section, we will introduce some novel studies on fabricating 3D materials via vapor deposition polymerization (VDP).

3.1 Homogeneous Film and Structure

The surface tension increases the difficulty of fabricating uniform membranes on geometric surfaces via liquid-phase polymerization. VDP removes the restrictions assessed by solvent surface tension. Tenhaeff's group reported that the film thickness uniformity on the top, sidewall, and bottom was better when the polymer was coated in the trench via CVD vs. liquid-phase polymerization.[150,151] On this merit, VDP could fabricate conformal membranes on topographically complex surfaces, such as patterned surfaces,[141] microtubes,[152] microchannels,[153] particles,[154] and woven fibers.[155–159] Figure 3A-i shows the conformal coating on the patterned substrate. The feature of diffusing reactants in the vapor phase allows VDP to fabricate conformal membranes in small geometries. The surface in the porous membrane of nylon was modified by poly(perfluorodecyl acrylate) (PPFDA) and PDVB via iCVD to improve the hydrophobicity.[39] A virus-structure surface was coated with polytetrafluoroethylene (PTFE) via iCVD to achieve continued superhydrophobicity without degradation for several months.[40]

A polymer membrane could be fabricated with nano- and microtopography by controlling the CVD polymerization conditions.[41] The poly(perfluorodecyl acrylate-co-ethylene glycol diacrylate) (p(PFDA-co-EGDA)) film polymerized via iCVD on the plasma-etched copper showed a nanoworm-like structure.[160] In the following paragraph, we focus on fabricating polymer film with nano- and microtopography on a flat substrate.

Gupta's group combined conventional and nonconventional iCVD processes to fabricate poly(methacrylic acid) (PMAA) membranes with pillared structure surfaces. First, the monomer was deposited in a sequential process. Then, the polymerization was subsequently controlled by turning on the filament. This combined process was also used to coat dense and porous membranes with PDVB and poly(methacrylic acid-co-methacrylic anhydride) to fabricate hydrophobic and hydrophilic membranes.[161]

Demirel's group used oblique angle VDP to fabricate thin films of poly(chloro-*p*-xylylene), poly(bromo-*p*-xylylene), and poly(o-trifluoroacetyl-*p*-xylylene-co-*p*-xylylene) with columnar nanostructures, shown in Figure 3A-ii. For oblique angle deposition, a titled flux assisted the deposition process at an oblique angle.[87,88] By changing the monomer for polymerization and the oblique angle, the chemical properties and film morphology of the nanostructured PPX membrane could be controlled at the same time. A two-layer PPX membrane could be fabricated readily by changing the oblique angle during the deposition process.[162] A columnar membrane was fabricated on a planar membrane when the oblique angle was changed from 90° to 10°.

Wei et al. fabricated a free-standing and patterned parylene C membrane with a columnar structure via a sequential

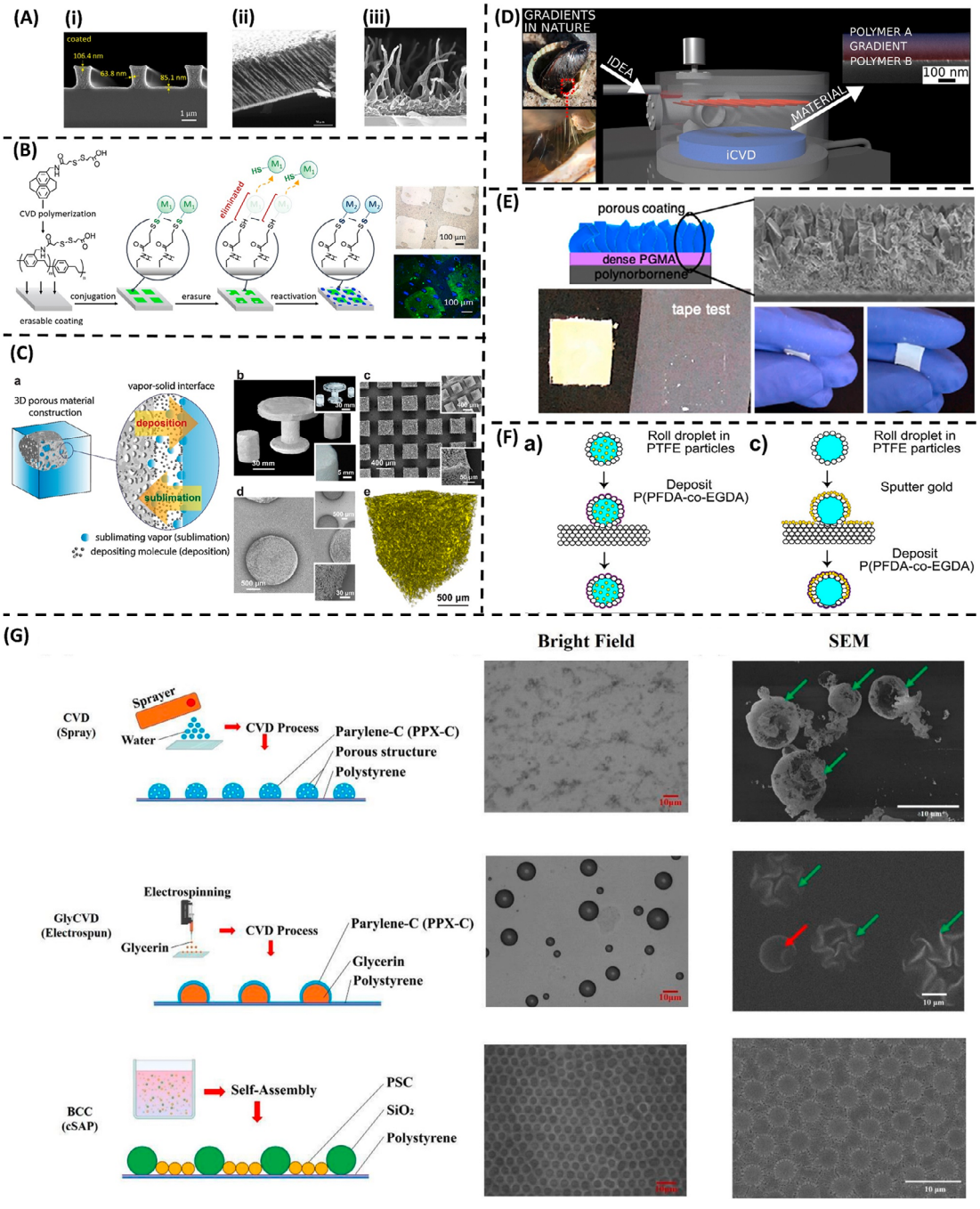

Figure 3 Manufacturing an anisotropic structure. (A) Surface structure: (i) cross-sectional SEM images of a conformal coating on a patterned substrate.[141] Reprinted with permission from Ref. 141. Copyright 2018 American Chemical Society. (ii) Cross-sectional SEM images of a columnar structure.[88] Reprinted with permission from Ref. 88. Copyright 2007 American Chemical Society. (iii) Side-view SEM images of a worm structure.[42] Reprinted with permission from Ref. 42. Copyright 2022 John Wiley and Sons. (B) Schematic diagram of patterning a surface via microcontact printing.[142] Reprinted from Ref. 142 published under a creative commons license (CC BY). (C) Schematic diagram of the fabrication of 3D porous materials by chemical vapor sublimation and deposition.[143] Reprinted with permission from Ref. 143. Copyright 2017 Elsevier. (D) Schematic diagram of a nanoscale gradient copolymer.[37] Reprinted with permission from Ref. 37. Copyright 2020 Elsevier. (E) A compartmentalized membrane.[51] Reprinted with permission from Ref. 51. Copyright 2020 American Chemical Society. (F) Schematic diagram of producing composite nanoparticles.[144] Reprinted with permission from Ref. 144. Copyright 2018 American Chemical Society. (G) Scheme of the fabrication of a granular structured membrane.[105] Reprinted from Ref. 105 published under a creative commons license (CC BY).

seven-step procedure.[89] A dense thin film of arylene C was polymerized on a patterned substrate, which was framed with thermal release tape. Then, a columnar parylene C film was polymerized on the dense film via vapor deposition with a vapor incidence angle of 5°. After heating, the compartment membrane was separated from the wafer.

Daniel Schwartz synthesized a PPFDA membrane with a worm structure on a silicon substrate via iCVD to achieve superhydrophobicity and superomniphobicity.[42] The micro- and nanoworms of PPFDA were directly constructed on planar silicon because of crystallization-directed nucleation and growth. The PPFDA membrane with worm-like structure is shown in Figure 3A-iii.

A superhydrophobic membrane of P(PFDA-co-EGDA) with a cone structure was polymerized on a polyethylene glycol diacrylate (PEGDA) membrane via iCVD.[43,163] While the partial pressure of PFDA in the chamber was above the saturation pressure of PFDA, the PFDA monomer was supersaturated on the PEGDA surface and nucleated to form nuclei as nanodroplets. Then, the PFDA monomer was adsorbed and polymerized on the cores to build a conical structure. Then, the PFDA monomer was adsorbed and polymerized on cores to build a conical structure, shown in Figure 3A-iii.

Wei et al. investigated iCVD on various liquid surfaces with a range of refractive indices.[44] A poly(perfluorooctyl methacrylate) membrane with a lens-structured protrusion formed on the liquid with a low refractive index because of the attractive long-range van der Waals interactions. In contrast, due to the repulsive van der Waals forces, discrete particles formed on the liquids with higher refractive indices under slow deposition. Robert et al. fabricated a spontaneous self-wrinkling film of poly(perfluorodecyl acrylate) via iCVD on a liquid-filled patterned surface.[164] The surface curvature of the polymer film was affected by the patterned substrate and the liquid filled in the patterned surface.

3.2 Patterned Structure

In recent years, researchers have devoted more effort to creating topological patterned surfaces to satisfy applications, including biotechnology and electronics. Fabricating patterned surfaces with masks during VDP could simultaneously obtain chemical and topological patterns. In 2007, Lahann's group reported vapor-assisted micropatterning in replica (VAMPIR) structures to fabricate chemically and topologically designable membranes of poly(4-pentafluoropropionyl-*p*-xylylene-co-*p*-xylylene),[165] poly(4-ethynyl-*p*-xylylene-co-*p*-xylylene),[166] poly(4-formyl-*p*-xylylene-co-*p*-xylylene),[166] poly(2,5-lutidinylene-co-*p*-xylylene),[167] and poly(4-ethynyl-2,5-lutidinylene-co-*p*-xylylene)[167]. In this method, monomers are deposited and polymerized on the area not covered by the replica structure during CVD polymerization. VAMPIR provides a straightforward way to pattern surfaces for selectable immobilization with fluorescence-labeled proteins or quantum dots.[165] The patterned surface via VAMPIR with functional parylenes undergoes bio-orthogonal multiple click chemistry reactions to immobilize various biomolecules.[166–169] A patterned hydrogel was efficiently fabricated via a successive process of polymeric initiator coating with a mask and SI-ATRP.[170]

3D structures can be formed using masks as well. Nathan J. Trujillo combined the principle of colloidal lithography and iCVD to fabricate patterned films with bowl structures.[45] A 2D colloidal monolayer assembly was templated first, followed by iCVD. After sonicating the film in a solvent, the colloidal template was moved from the patterned film. Different functions could be achieved by using different monomers for iCVD to fabricate patterned membranes with organic polymers (PBA and PHEMA), fluoropolymers (PPFDA and PPFM), and organosilicones (PV4D4).

Select polymerization with an inhibitor or inducer could also produce a patterned surface. Microcontact printing (μCP) is a common technique for patterning flat surfaces with elastomer stamps and can assist in pattern fabrication under vapor deposition coating processes. F. Bally immobilized various bioactive molecules via μCP on a poly(4-ethynyl-*p*-xylylene-co-*p*-xylylene) membrane fabricated via CVD polymerization.[168] The excellent selectivity of cell adhesion on the partially immobilized cell-adhesion peptide indicates efficient patterning and the specific click chemistry reaction.[168] Through μCP of molecules with an erasable group, a second functional group could be printed after removing the terminal group on the first patterned molecule.[142] The scheme for μCP and immobilization is shown in Figure 3B. An inhibitor could exclude polymer growth on the designed locations to produce a patterned film. For example, Kahp et al. fabricated parallel channels with a selectively polymerizing membrane on the sidewall via CVD polymerization by inhibiting polymer growth with an iron coating.[171]

The conventional method for patterning with a mask or stamp has difficulty in applying to non-flat surfaces. Thus, some novel techniques were designed to directly coat patterned films. VDP-mediated inkjet-printed polyaniline (VDP-IJP) was reported to efficiently pattern polymers on a flexible substrate (poly(ethylene terephthalate), PET) with micrometer-scale resolution by Jyongsik Jang's group.[79,80] In the VDP-IJP procedure, the oxidized ink was printed on the substrate to induce oCVD.[78] After immobilizing RGD on VDP-IJP patterns, the pattern exhibited good selectivity for cell growth and detecting neurotransmitters.

Some researchers have utilized photolithography to fabricate patterned surfaces with photoactive polymers, photodefinable polymers, and polymers that can be photosynthesized. Multilayered methyl methacrylate and styrene patterns were built via vapor-phase-assisted surface photopolymerization (photo-VASP) with a stripe-patterned pho-

tomask on a Si wafer and Au plate.[172] The patterned polymer film could be autodrawn under photo-VASP with a computer program. The polymerization of *N*-isopropylacrylamide (NIPAAm), styrene, and acrylic acid (AA) could be conducted at different areas separately by changing the monomer and X – Y stages.[173] The photoactivity of the polymer could also be used to produce patterns after the polymer film was coated. Utilizing the photoactivity of PPMA, a pattern could be provided by using e-beam irradiation.[138] The other method is fabricating the polymer with a phototrigger-clickable functional group.[90] Colloidal particles with broad-range patterns were fabricated by a two-step procedure of photodefinable PPX coating via CVD polymerization and photoreactive coating with projection lithography through a digital micromirror device.

3.3 Porosity and Gradient

Resorting to the conformal coating of VDP, a porous membrane can be produced by coating the polymer on a porous scaffold as a template. For example, porous (PPX) foam was fabricated by CVD polymerization on spongy sugar cubes.[91] One-step VDP of acrylonitrile on colloidal silica particles was conducted to fabricate silica-polyacrylonitrile composites.[174] Mesoporous carbon was obtained after removing the silica particles and carbonization.

In recent years, many studies have been dedicated to achieving nanostructure surfaces by altering the polymerization processes. Gupta's group provided a procedure of iCVD to fabricate a porous polymer membrane of PMAA by tuning the partial pressure of the monomer and the tempura structure.[46] Scott Seidel reported a two-step process of fabricating porous membranes of PMMA: (1) vapor deposition of the monomer and (2) filament cleaving of TBPO and PMMA polymerization. The sublimation of unreacted monomer led to porous structure formation. They reported that the membrane structure was affected by physical monomer deposition, which was controlled by the monomer flow rate and the substrate temperature. The low temperature of the substrate reduced the surface diffusion of MMA, causing an increase in the shadowing effect to form a sponge-like membrane.[41,47,48] An asymmetric membrane of poly(1,3,5,7-tetravinyl-1,3,5,7-tetramethylcyclotetrasiloxane-co-ethylene glycol diacrylate) (p(V4D4-co-EGDA)) was produced on silicone oil via iCVD. The bottom surface, which was near the oil side, had greater porosity. The top surface was packed densely and loosely in terms of topography. Increasing the V4D4 content in the copolymer increased the porosity and microstructure regions.[49]

Matsumoto's group provided a technique for producing porous polyurea (PU) via vacuum deposition polymerization with the ionic liquid (IL) of 1-ethyl-3-methylimidazolium bis (trifluoromethylsulfonyl) amide ([Emim][TFSA]). A porous PU film was copolymerized by depositing 4,4′-methylene-bis(2-chlorophenyl isocyanate) and 2,7-diaminofluorene monomer molecules on the IL-coated substrate.[175,176] The reversibility of IL deposition and vacuum annealing in the PU pores provided rewritable ion conduction.[177]

Adding porogen to change the mass transfer has been used to fabricate porous structures. Mixing ethylene glycol as a porogen into a gas mixture of monomer and crosslinker simultaneously combined VDP with phase separation to fabricate a porous poly(glycidyl methacrylate) (PGMA) film when the saturation degree of the monomer and porogen surpassed unity. The concentrations of the crosslinkers and porogens in the gas phase and the reactivity of the monomers controlled the size, density, and morphology of the pores. A layer-by-layer membrane with a dense and porous film could be fabricated by changing the feed-in flow under VDP.[178] The relationship between pore morphology and porogen type has been discussed in earlier studies.[179,180] The membrane morphologies of sphere agglomeration, unconnected sheets, and crater-like shapes were observed when a highly immiscible liquid porogen, a highly immiscible and crystallizable porogen, and the most miscible porogen were used, respectively.

However, in previous reports, a porous structure could only be fabricated in a polymer membrane. Chen's group developed a novel method with only one step to fabricate porous membranes and 3D particles. They developed a unique method to fabricate porous, asymmetrical, and gradient PPX membrane structures via chemical vapor sublimation and deposition (CVSD). The diradical deposition on the subliming surface of the ice template formed a porous structure.[92] Figure 3C shows the scheme for CVSD and the images for the porous materials. This technique showed remarkable controllability for making structural and functional asymmetry and gradients at multiple scales. Functionalized porous PPX membranes of poly[(4-*N*-maleimidomethyl-*p*-xylylene)-co-(*p*-xylylene) and poly((methyl propiolate-*p*-xylylene)-co-(*p*-xylylene)) were produced via CVSD.[93,94]

Physical and chemical gradients are selective in some specific applications, such as selective cell differentiation. Here, we introduce some techniques and processes to produce a gradient polymer membrane. A 2D morphological and compositional gradient film of parylene C was fabricated via a two-step process of oblique angle CVD and oxygen plasma treatment.[95] First, a parylene C film was deposited via oblique angle CVD on a columnar thin film to fabricate a morphological gradient along the length. Then, each row's surface was treated by oxygen plasma at a different time to produce a hydrophilicity gradient. The thickness gradient of the polymer was fabricated by sequentially evaporating a shutter and a sliding mask under VDP.[96,97]

Via CVSD polymerization, a porosity gradient and a multifunctional gradient were provided by designing the composition of the ice template.[92] A PPX membrane with a po-

rosity gradient was fabricated by CVSD polymerization on an ice template made from a gradient solution of ethanol/water. The gradient composition of ethanol in the template provided a volatility gradient to produce the porosity gradient. The deposition polymerization produced the parallel gradient function of physical magnetic and chemical electrochemical conductivity on the template with a gradient composition of Fe_3O_4 and PEDOT.

Yaseen Elkasabi et al. fabricated a surface composition gradient from two functionalized monomers of [2.2]paracyclophane (4-trifluoroacetyl[2,2]paracyclophane and 4-aminomethyl[2,2]paracyclophane) via CVD copolymerization.[9] Two monomers were fed into the system from the inlet on the opposite side. When the two sources flowed into the chamber, the monomer was gradually depleted, and the monomer composition decreased in the gas phase. The monomers with a gradient composition in the gas deposited and polymerized. Based on this technique, Elkasabi fabricated composition gradients with CHO and NH_2 groups to immobilize biotin hydrazide and sulfo-NHS-LC-biotin to produce cellular transduction gradients.[181] The assistance of a PDMS channel with a metal baffle reduced the compositional slope of the gradient and made gradient coatings for 3D objects possible.[182] By programming the gradual change of the monomer concentration of 1,3,5-trivinyl-1,3,5-trimethylcyclotrisiloxane (V3D3) and 1H,1H,2H,2H-perfluorooctyl acrylate (C6PFA) or hexafluoropropylene oxide (HFPO), a vertically gradient polymer membrane was fabricated with a nanoscale gradient via CVD.[37] The scheme for producing gradient copolymer materials is shown in Figure 3D. The compositional gradient of PV4D4 and the polyampholyte poly(2-carboxyethyl acrylate-co-2-(dimethylamino)ethyl acrylate) (PCD) was fabricated via iCVD by controlling the flow rate of monomers.[50] The flow rate of V4D4 was decreased over the processing time, while the flow rate of PCD was increased.

3.4 Polymer Compartmentalization and Composites

VDP can compartmentalize polymer films by layer-by-layer polymerization without other treatment. The physical and chemical properties can be controlled by changing the monomer, substrate, and processing parameters. An asymmetric bilayer membrane consisting of a sponge layer and a dense layer with a pillared structure surface was polymerized under different processing conditions with various monomers via iCVD.[48] A free-standing membrane (FSM) comparting with the dense film and fibrous film of parylene-C, which was polymerized via iCVD, was fabricated by a seven-step procedure.[89] Ran et al. fabricated a compartment GMA membrane with a dense and porous structure by layer-by-layer coating with simultaneous phase separation during CVD.[178]

By designing the processing conditions and monomer, asymmetry in both the structure and chemical properties can be obtained simultaneously.[161] A porous membrane from MAA, ethylene glycol diacrylate (EGDA), and GMA was coated on a dense PGMA membrane via iCVD to improve the scratch resistance and solvent resistance, and the dense PGMA layer promoted adhesion between the porous membrane and substrates.[51] The layer-by-layer compartmentalized membrane is shown in Figure 3E. A bilayer coating of a highly crosslinked PEGDA bottom layer and nanostructured P(PFDA-co-EGDA) top layer was fabricated by a two-step deposition process via iCVD to increase the surface hydrophobicity.[43]

VDP can be used to fabricate layer-by-layer membranes on 3D substrates. For example, coaxial nanotubes with a hydrogel core and a shape memory shell were demonstrated by coaxial vapor deposition of poly(*tert*-butyl acrylate) and PHEMA, respectively, in an anodic aluminum oxide (AAO) template.[183]

A polymer membrane with compartments was fabricated via VDP. Chen's group provided a multicomponent vapor-deposited porous (MVP) coating of functional poly-(*p*-xylylene) based on CVSD polymerization to fabricate various compartments.[98,99] This method increases the versatility of making different multicomponent coatings with asymmetric structures and chemical properties. It is worth mentioning that an asymmetric hybrid coating of a porous particle-capsulated membrane could be produced via the MVP coating. By making the ice template with different molecules or cells, cell adhesion and differentiation were successfully controlled.[100–102]

For some applications, the composite material is necessary to maintain the physical or chemical properties that the application needs. Here, we introduce some composite membranes or particles produced via VDP. Poly(*N,N*-dimethylaminoethyl methacrylate-co-ethylene glycol dimethacrylate) (P(DMAEMA-co-EGDMA)) was iCVD-polymerized on candle soot (CS).[52] The CS@polymer composites were used as humidity sensors with outstanding humidity sensing performance. Mark et al. fabricated two types of composite particles with inorganic nanoparticles by combining iCVD and direct-current magnetron sputtering. The scheme for procedures is shown in Figure 3F. First, a low-vapor liquid with embedded gold nanoparticles was capsuled with PTFE particles, which enhanced the mechanical strength of the marble. Then, the spherical marbles were vapor-deposited and polymerized with PPFDA or gold nanoparticles were deposited before PPFDA deposition polymerization.[144] PPY was vapor-deposited and polymerized onto waste Si as the pre-product for the N-doped carbon source. After carbonization, Si/N-doped carbon core-shell composites were fabricated and provided a lower barrier of Li-ion transport energy.[184] Polyaniline was conformally coated on carbon nanotubes via oCVD at a low deposition temperature.[81]

Two-layer hybrid nano- and mesotubes were fabricated by deposition polymerization of PPX and metal on degradable template polymer fibers (PLA, poly(L-lactide)) via subsequent CVD.[103] A hybrid nanocomposite with graphene, dopamine, and PPY was fabricated for flexible supercapacitor electrodes by coating PPY on dopamine-loaded graphene.[82]

3.5 From 2D to 3D

AAO templates are a standard tool for fabricating nanotubes. By VDP, nanotubes with different polymers, such as PEDOT[83] and PPy[84], were made. Carbon nanotubes were produced after carbonizing the PPy nanotubes, which were fabricated by VDP on an AAO template.[84] Coaxial nanotubes have been manufactured by sequence iCVD on an AAO template with temperature-responsive poly(*N*-isopropylacrylamide) (PNIPAAm), pH-responsive PMAA and PHEMA.[53] Ozaydin Ince's group also reported various polymer nanotubes made from iCVD or oCVD with AAO templates.[183,185–187] By using the fiber template process (TUFT), PPX nanotubes and metal–PPX hybrid nanotubes were fabricated.[103] PPX was first coated on degradable polylactic acid (PLA) template polymer fibers. After removing the PLA fiber, a hollow tube of PPX was obtained. Combined with metal deposition, a core-shell tube was fabricated.

Poly(4-vinylpyridine) and PHEMA polymer particles were polymerized in silicone oil via sequential CVD.[54] The monomer was first condensed on the oil surface and then polymerized via a free radical reaction. Chen's group reported a novel method to fabricate porous particles with various structures and sizes via CVD.[93,104] The particle size can be controlled by tuning the sublimation/deposition process.[104] More importantly, particles with growth factors, platelet-rich plasma, or live cells were directly encapsulated in the membrane by VDP. This compartmentalized membrane has been utilized to control cell growth.[100–102]

Franklin's group fabricated nonspherical polymer nanoparticles (PNPs) by condensed droplet polymerization, which is similar to iCVD.[188] The nanoscale droplets were condensed on the PPFDA from the vapor-phase monomer of HEMA firstly, then the free radical initial polymerization occurred after the vapor-phase initiator (TBPO) was fed into the heated chamber (300 °C). The authors point out that the shape, size, and intensity of PNPs could also be alternated by using various monomers, tuning the surface energy of the base layer.

By depositing monomers on a drop of liquid, a curved polymer membrane could be fabricated. This year, Yung-Chiang Liu et al. fabricated hybrid granular structures of parylene C, a polystyrene layer, GlyCVD particles, SiO_2, and carboxylated polystyrene particles by combining colloidal self-assembly and CVD.[105] The processing illustration is shown in Figure 3G. By depositing the polymer on a glycerin drop, a granular structure membrane of parylene C was obtained. After 5 days of incubation, human bone marrow mesenchymal stem cells aggregated without a reduction in the cell activity.

Transformable compartmentalized microstrips, which can reversibly change the structure between 2D and 3D, have been produced via VDP. Myung Seok Oh et al. demonstrated Janus microstrips by coating PDVB on active microstrips.[55] The active microstrips were photopolymerized from PHEMA, poly((ethylene glycol) diacrylate), AA, and the photoinitiator 2-hydroxy-2-methylpropiophenone. Then, the Janus property was provided by the iCVD coating PDVB layer, which was not responsive to pH changes. While increasing pH condition, the pH-responsive AA-containing microstrip swelled, resulting in directional self-bending. The self-bending degree was affected by the thickness changes of the active layer and passive layer, and a 3D microstructure was formed under high pH conditions.

4. Applications

Synthesized polymers have been widely applied to surface modification and membrane fabrication. Here, we discuss surface modification and membrane formation.

4.1 Surface Modification Coatings

Surface modification for various applications can be satisfied by proper coating polymers to utilize the surface physicochemical properties. Controlling surface hydrophilicity and hydrophobicity has drawn much interest in antibacterial,[189–191] corrosion resistance,[192–194] drug delivery,[195] gate dielectric,[69] and electrolyte[177] applications. The surface of a porous ceramic tube was modified into a hydrophobic surface with PPFDA via iCVD to enhance the performance of membrane distillation by limiting membrane wetting.[196] The polymer film also impacted droplet shedding and decreased the contact angle. PEDOT was coated on layered oxide cathode materials via oCVD to improve the capacity and thermal stability under high-voltage operation.[85] P(DMAEMA-co-EGDMA) was coated on a CS film via iCVD.[52] The polymer@CS composite was highly hydrophilic and had good sensitivity when used as a humidity sensor. The PNIPAAm, which is sensitive to humidity, was coated on an optical cavity via iCVD to demonstrate a humidity sensor.[56] An iCVD-polymerized gradient membrane of PV4D4 and PCD provided good antifouling properties with the outer layer of pCD and strong substrate-independent adhesion of PV4D4.[50] Poly(dimethyl amino methyl styrene-co-1H,1H,2H,2H-perfluorodecyl acrylate) (P(DMAMS-co-PFDA)) was modified on the negatively charged and hydrophilic surface of polyester textile via iCVD to provide anti-

fouling properties.[57] The schematic diagram of the coating process and antifouling is shown in Figure 4A. The hydrophobic PDP membrane exhibited excellent killing efficiency against gram-negative *Escherichia coli* and gram-positive methicillin-resistant *Staphylococcus aureus*.

Zwitterionic polymers are commonly used in antifouling applications. The iCVD polymerized 2-hydroxyethyl methacrylate-co-perfluorodecyl acrylate (HEMA-co-PFDA), a zwitterionic copolymer, also exhibited good resistance to organic fouling for assisting a reverse osmosis (RO) membrane.[58] Poly[2-(dimethylamino)ethyl methacrylate-co-ethylene glycol dimethacrylate) (PDE) was coated on a RO membrane via iCVD, and the zwitterionic structure was obtained by reacting with 1,3-propane sultone. Then, the zwitterionic membrane was crosslinked with EGDMA to prevent dissolution in water.[59]

Providing a specific interface with nanomembranes has played an important role in biotechnology. Various surface properties can be obtained using different polymer coatings to achieve applications. Poly(methylacrylic acid-ethylene glycol diacrylate) (P(MAA-EGDA)) was coated on a PLA membrane to improve the hemocompatibility.[60] The negative carboxyl groups on P(MAA-EGDA) were hydrophilically interacting with protein and platelets and electrostatically interacting with the amide groups of thrombin to inhibit clotting.[60] A composite patch was modified with poly(2-hydroxyethyl methacrylate-co-ethylene glycol dimethacrylate) (P(HEMA-co-EGDMA)) via iCVD to improve wettability and biocompatibility and exhibited good cell interaction with human osteoblasts.[61] The composite patch and fluorescence imaging of human osteoblasts at 48 h culturing are shown in Figure 4B. By coating the biocompatible poly(ethylene glycol dimethacrylate) (PEGDMA) via iCVD, the mor-

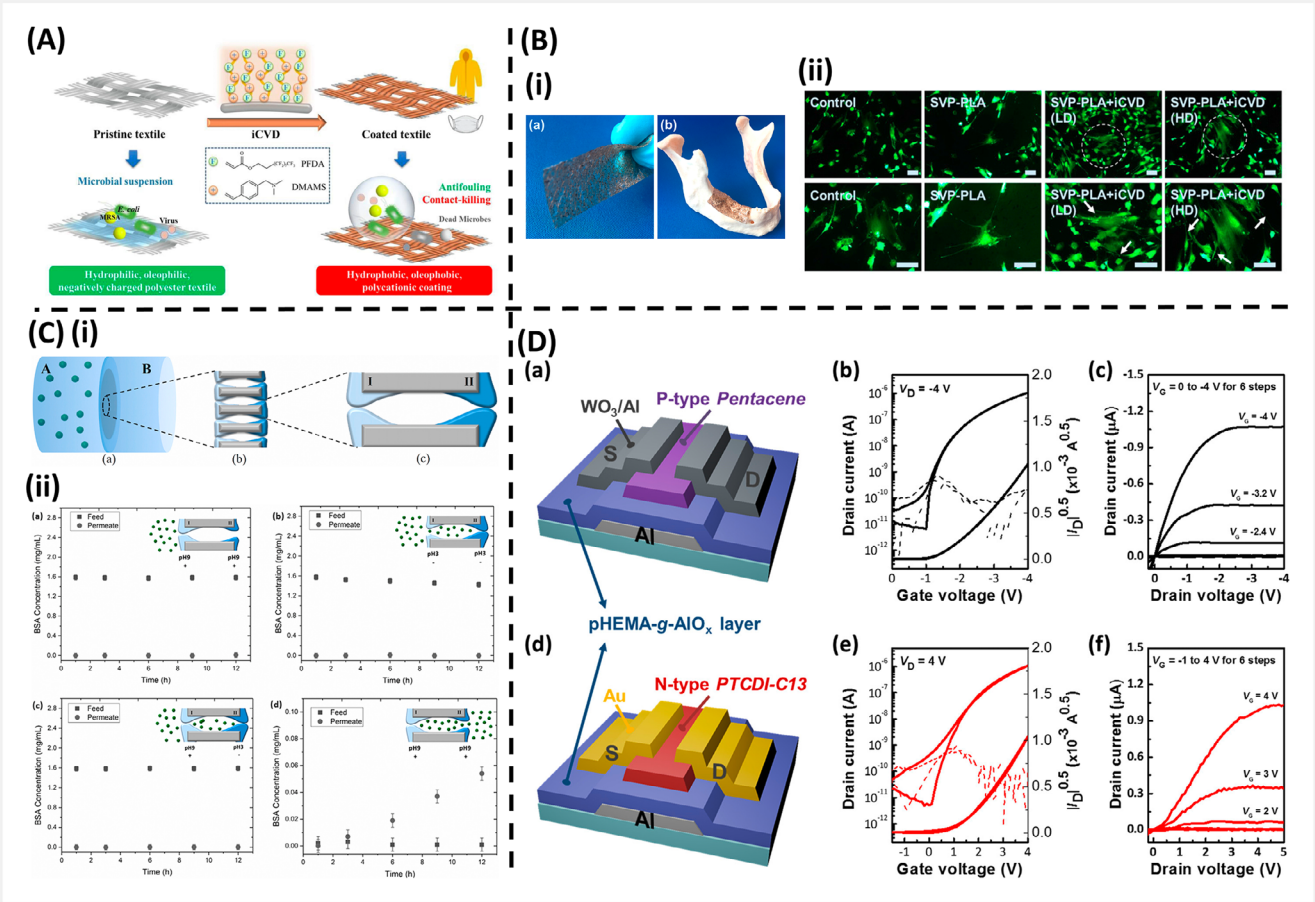

Figure 4 Surface modification. (A) Schematic diagram of the iCVD process for antifouling application.[57] Reprinted with permission from Ref. 57. Copyright 2021 Elsevier. (B) P(HEMA-co-EGDMA)-coated SVP-PLA composite patch: (i) composite patch and (ii) fluorescence imaging of human osteoblasts on the composite patch and copolymer-coated patch[61] (scale bar = 20 μm). Reprinted from Ref. 61 published under a creative commons license (CC BY). (C) pH-responsive Janus membrane: (i) illustration of the Janus membrane and (ii) the cumulated BSA concentration in the feed and permeated cells.[68] Reprinted with permission from Ref. 68. Copyright 2019 Elsevier. (D) The scheme of a hybrid dielectric and the device performance.[69] Reprinted with permission from Ref. 69. Copyright 2018 American Chemical Society.

phology durability of gelatin nanofibers was improved without losing cytocompatibility.[158] A hybrid polyionic nanocoating was fabricated by two-stage iCVD to graft polyionics onto a polyionic poly(2-dimethylamino ethyl methacrylate-co-methacrylic acid-co-ethylene glycol diacrylate) (PDME) membrane on neural microelectrodes to reduce microglial adhesion and adsorption of laminin and bovine serum albumin (BSA).[62]

A hydrogel copolymerized from HEMA and EGDMA can change the indomethacin release behavior by changing the composition of EGDMA.[63] When the EGDMA content increased, the crosslinker fraction increased, and the release rate decreased. The hydrogels PHEMA and PMMA were coated on clotrimazole (CLOT)-loaded cotton, PET fabrics, or polycaprolactone nanofibers via iCVD, which prevented sudden drug release.[64]

Stimuli-responsive polymers can change properties by altering the environmental conditions, such as pH, temperature, and water exposure. These properties can be used in providing drug delivery, controlling permeation, and fabricating cell sheets. A thermoresponsive poly(*N*-vinylcaprolactam) (PNVCL) surface was fabricated via iCVD on glass to provide the surface with alterable hydrophilicity to thermally separate the cell sheet by lowering the temperature.[65] Degradation and swelling could also be utilized for drug release. The pH-dependent degradable poly(methacrylic anhydride) (PMAH) was coated via iCVD to capsulate a drug within the microporous membrane.[66] The drug release rate was controlled by the degradation of PMAH resulting from the pH increase. PMAA also showed good pH responsiveness to control drug release by polymer swelling.[51] By polymerizing MAA, an epoxide-containing monomer (GMA), and a crosslinker (EGDA) via iCVD, a robust porous polymer membrane for drug delivery and wound dressing was fabricated. The pH-sensitive poly(methylacrylic acid-co-ethylene glycol dimethacrylate) (p(MAA-co-EGDMA)) was conformally coated in the pore walls of AAO templates via iCVD. The pore size change due to pH-responsive swelling controlled the permeation rate of molecules.[67] Different pH-responsive polymers were coated in the pore walls at opposite sides of the AAO templates via iCVD. The polymer-coated pores acted as controllable gates at the opposite sides to block the molecular permeation individually.[68] The schematic of the Janus membrane and the protein concentration change in the feed and permeated cells are shown in Figure 4C.

Coating with a specific polymer can also promote the performance of applications. Coating the poly(hydroxyethyl methacrylate-co-ethylene glycol diacrylate) (poly(HEMA-co-EGDA)) hydrogel electrolyte via iCVD on a patterned nanostructure can be applied for 3D microbatteries.[141] The hydroxyl groups in the HEMA component promoted strong interactions with anions, resulting in lithium salt dissociation enhancement. A homogenous organic–inorganic hybrid membrane was vapor-deposited and polymerized from TMA, the vinyl monomer HEMA, and the initiator TBPO via iCVD polymerization.[69]

The performance of the device with hybrid dielectric and the illustration of hybrid dielectric are shown in Figure 4D. The organic thin-film transistors with the designed hybrid dielectrics exhibited excellent flexibility and good dielectric performance. The heat transfer coefficient of a vapor-side condenser was successfully enhanced by coating poly-(1H,1H,2H,2H-perfluorodecyl acrylate)-co-divinyl benzene (p(PFDA-co-DVB)) on the metal tube.[202] VPP can be utilized to connect fibers. For instance, macroscopic graphene composite webs were fabricated by CVD of polymerized polyacrylonitrile (PAN) on PAN fibers.[156] After carbonizing fibers at a high temperature (1000 °C), the PAN polymer was carbonized with sp^2-hybridized carbon atoms in the macroscopic graphene composite webs. The graphene composite webs reveal outstanding electrical conductivity. PHEMA was modified in mesoporous TiO_2 via iCVD as a polymer electrolyte.[203] The efficiency of electrolyte dye-sensitized solar cells was enhanced compared to that of liquid-filled devices, while PHEMA formed a stable gel electrolyte.

4.2 Membranes

Free-standing polymer films have been applied as filters, tissue scaffolds, and drug delivery systems. A heat or solvent-removable layer is coated on the holder before VDP. Below are some examples of CVD-polymerized free-standing films.

Five millimeter thick polymeric FSMs of nBA were fabricated by iCVD and crosslinked with diethylene glycol divinyl ether (DEGDVE).[204] After dissolving the poly(acrylic acid) (PAA) layer, FSMs were obtained and combined in a microfluidic device and showed 1.3 times the CO_2 permeance compared to the control membrane.

A PHEMA FSM was fabricated via iCVD and is shown in Figure 5A.[197] The hydrophilic molecules showed a higher permeability coefficient because of the polarities. The crosslinking ratio of the membrane affected the diffusion coefficient. Jyun-Ting Wu et al. produced a prototype of a PPX intraocular lens (PPX-IOL) device with functionalized PPXs via CVD encapsulation.[198] Figure 5B shows the scheme of fabrication process and the image of prototype PPX-IOL. During CVD encapsulation, the polymer was deposited on the placed liquid droplet and polymerized. After photoimmobilization with thiol-PEGs and cysteine-containing peptides, the PPX-IOL devices showed cell resistance and cell attachment.

4.3 Device Fabrication

VDP has the advantage of preparing pure and conformal membranes on various substrates. By combining with other

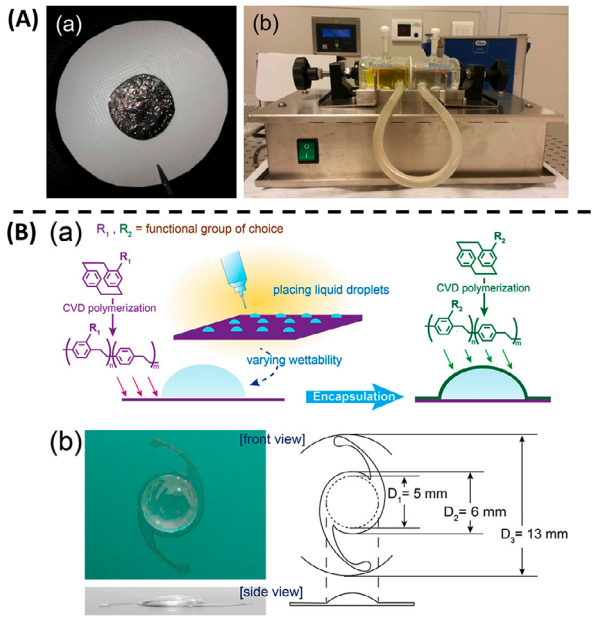

Figure 5 Free-standing membrane fabrication. (A) PHEMA membrane and the diffusion cell for the permeation test[197] Reprinted with permission from Ref. 197. Copyright 2014 John Wiley and Sons. (B) Schematic diagram of fabricating poly-*para*-xylylene (PPX) intraocular lens and the image of PPX intraocular lens[198] Reprinted with permission from Ref. 198. Copyright 2015 American Chemical Society.

techniques, such as functionalization, VDP has been employed as a modification process for producing devices, such as electric devices, biomedical devices, and sensors. For example, iCVD was used to fabricate a conformal copolymer in a microfluidic sensor. Jung et al. produced DNA hydrogels by the isothermal amplification of complementary target (DhITACT) system in a microfluidic channel with an iCVD-coated copolymer (Figure 6A).[199] PV4D4 was conformally modified in the channel. It needs to be emphasized that the iCVD process can directly modify the inside wall of microfluidic channels without pretreatment and coat a large number of devices at once. Then, the copolymer-coated channel was immobilized with DNA primer via a thiol-end click reaction. The DhITACT system showed rapid diagnosis with high sensitivity for MERS (Middle East respiratory syndrome) coronavirus.

Recently, the iCVD has been used to coat ultra-thin polymers for producing organic/inorganic hybrid dielectrics with good performance.[200] A scheme of hybrid dielectric fabrication is shown in Figure 6B. Poly-2-hydroxyethyl methacrylate-co-1,3,5-trivinyl-trimethyl-cyclotrisiloxane (PHEMA-co-V3D3) was coated on a Ni bottom electrode in a resistive random access memory (ReRAM) device via iCVD, and the copolymer-based ReRAM device showed high endurance properties.[201] The PV3D3 dielectric was found to

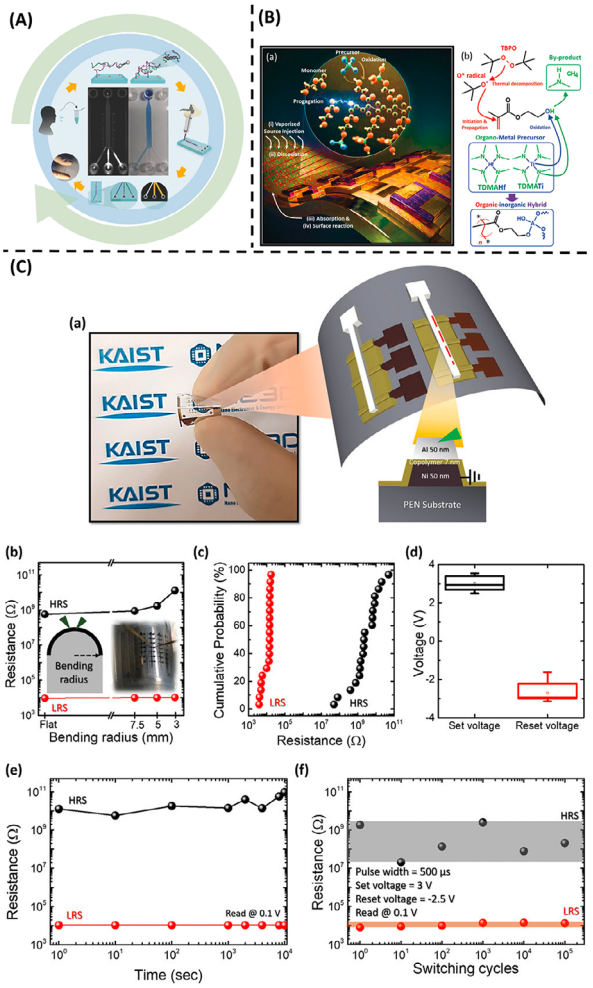

Figure 6 Vapor deposition polymerization for device fabrication. (A) Microfluidic device for target virus detection.[199] Reprinted with permission from Ref. 199. Copyright 2016 John Wiley and Sons. (B) Schematic diagram of hybrid dielectric synthesis.[200] Reprinted with permission from Ref. 200. Copyright 2021 John Wiley and Sons. (C) Copolymer-based ReRAM device and its stability test results.[201] Reprinted with permission from Ref. 201. Copyright 2021 John Wiley and Sons.

have a more stable and robust insulating property than the pHEMA dielectric, preventing soft breakdown behavior. The ReRAM device with the copolymer dielectric achieved both low switching power and high endurance characteristics. The copolymer ReRAM on flexible PEN and the performance under different bending radii are shown in Figure 6C.

5. Conclusions and Outlook

In vapor deposition, the coating component evaporates into atoms, molecules, or ions, which then condense on the sur-

face of the substrate. Vapor deposition is an excellent technique for fabricating insoluble or infusible polymer thin films such as fluoropolymers, crosslinked organic materials, and conjugated polymers. Unlike PVD methods such as sputtering or evaporation, which use atoms as the film-building species, CVD uses reactive molecules or radicals to fabricate polymeric films through a chemical reaction. The most common CVD variations used to fabricate polymer thin films are iCVD, piCVD, PECVD, oCVD, and parylene CVD. The thin film properties, such as thickness, surface morphology, and mechanical properties, vary depending on the vapor deposition process, monomers, and substrates used to construct it. However, the thin film functionalities are highly dependent on the functional groups of monomers. Covalent bonding, surface chemistry such as alkyne–azide "click" chemistry, and other chemical reactions are made possible by these functional groups. The control over these properties and functions is provided by the CVD technique, demonstrating that CVD is a versatile way to fabricate thin films that can be tailored to fit the needs. Nanotopography and a porous structure can be achieved by modifying the processing settings during deposition or combining other processing techniques. In addition, the patterning process has the capability of designing surfaces with anisotropic chemistry and topography for subsequent functionalization as modifications for specific purposes. Producing a gradient in terms of the chemical characteristics, thickness, and porosity of the material is possible with the assistance of other methods. In addition, 3D particles, tubes, and curved FSMs have also been constructed. Surface modification by VDP demonstrates its versatility for a wide range of applications after being compartmentalized with different types of materials. With the increasing demand and sophistication of the interface requirements for prospective materials, the capabilities of an interface modification tool (surface modification and/or a coating) are expected with (i) multiple functions from both physical and chemical aspects and/or their combined properties, (ii) controlled configuration and compositions of these physical and chemical properties from 2D to 3D and in selected locations (anisotropic control), (iii) increased compatibility with a wide spectrum of substrate materials and devices without compromising the fabrication process or the intended functionality, (iv) easy accessibility of the fabrication process, cost, and the possibility of mass production for industrialization applications, (v) sustainable presentation of the properties for prolonged cycles and usages, and (vi) combination of different coating techniques in a complimentary and combinatorial fashion. We expect the advancement of the vapor deposition and coating technologies of polymers to expand beyond the discussions, and new researchers in this field will benefit from this review and bring new insights into vapor deposition coatings in the future.

Funding Information

The authors gratefully acknowledge funding support from the National Science and Technology Council of Taiwan (111-2221-E-002-030-MY3; MOST 108-2221-E-002-169-MY3; 109-2314-B-002-041-MY3).

Conflict of Interest

The authors declare no competing conflicts of interest.

References

(1) Yang, R.; Asatekin, A.; Gleason, K. K. *Soft Matter* **2012**, *8*, 31.
(2) Yu, S. J.; Pak, K.; Kwak, M. J.; Joo, M.; Kim, B. J.; Oh, M. S.; Baek, J.; Park, H.; Choi, G.; Kim, D. H.; Choi, J.; Choi, Y.; Shin, J.; Moon, H.; Lee, E.; Im, S. G. *Adv. Eng. Mater.* **2018**, *20*, 1700622.
(3) Bazaka, K.; Grant, D. S.; Alancherry, S.; Jacob, M. V. *Plasma-Assisted Fabrication and Processing of Biomaterials*. In *Biomedical Applications of Polymeric Materials and Composites*. Francis, R.; Kumar, D. S., Wiley-VCH: Weinheim, **2016**, 91.
(4) Coclite, A. M. *CVD Polymer Surfaces for Biotechnology and Biomedicine* In *CVD Polymers: Fabrication of Organic Surfaces and Devices*. Gleason, K. K., Wiley-VCH: Weinheim, **2015**, 301.
(5) Sun, T.; Qing, G.; Su, B.; Jiang, L. *Chem. Soc. Rev.* **2011**, 40, 2029.
(6) Yoshida, M.; Langer, R.; Lendlein, A.; Lahann, J. *J. Macromol. Sci., Polym. Rev.* **2006**, *46*, 347.
(7) Lahann, J. *Polym. Int.* **2006**, *55*, 1361.
(8) Lahann, J. *Chem. Eng. Commun.* **2006**, *193*, 1457.
(9) Elkasabi, Y.; Lahann, J. *Macromol. Rapid Commun.* **2009**, *30*, 57.
(10) Elkasabi, Y.; Yoshida, M.; Nandivada, H.; Chen, H.-Y.; Lahann, J. *Macromol. Rapid Commun.* **2008**, *29*, 855.
(11) Tiefenauer, L.; Ros, R. *Colloids Surf., B* **2002**, *23*, 95.
(12) Sun, T.; Qing, G.; Su, B.; Jiang, L. *Chem. Soc. Rev.* **2011**, *40*, 2909.
(13) Langer, R.; Tirrell, D. A. *Nature* **2004**, *428*, 487.
(14) Tu, R. S.; Tirrell, M. *Adv. Drug Delivery Rev.* **2004**, *56*, 1537.
(15) Khademhosseini, A.; Langer, R.; Borenstein, J.; Vacanti, J. P. *Proc. Natl. Acad. Sci. U.S.A.* **2006**, *103*, 2480.
(16) Ross, A. M.; Jiang, Z.; Bastmeyer, M.; Lahann, J. *Small* **2012**, *8*, 336.
(17) Gao, Y.; Cole, B.; Tenhaeff, W. E. *Macromol. Mater. Eng.* **2018**, *303*, 1700425.
(18) Hassan, Z.; Varadharajan, D.; Zippel, C.; Begum, S.; Lahann, J.; Bräse, S. *Adv. Mater.* **2022**, *34*, 2201761.
(19) Elsabahy, M.; Heo, G. S.; Lim, S. M.; Sun, G.; Wooley, K. L. *Chem. Rev.* **2015**, *115*, 10967.
(20) Moni, P.; Al-Obeidi, A.; Gleason, K. K. *J. Nanotechnol. (Beilstein)* **2017**, *8*, 723.
(21) Bilger, D.; Homayounfar, S. Z.; Andrew, T. L. *J. Mater. Chem. C* **2019**, *7*, 7159.
(22) Yang, D.; Wanglin, C.; Bingxin, L.; Chengyong, W.; Tongchun, K.; Yanqiu, L. *Ceram. Int.* **2020**, *46*, 18373.
(23) Coclite, A. M.; Howden, R. M.; Borrelli, D. C.; Petruczok, C. D.; Yang, R.; Yagüe, J. L.; Ugur, A.; Chen, N.; Lee, S.; Jo, W. J.; Liu, A.; Wang, X.; Gleason, K. K. *Adv. Mater.* **2013**, *25*, 5392.
(24) Redka, D.; Buttberg, M.; Franz, G. *Processes* **2022**, *10*, 1982.
(25) Sun, L.; Yuan, G.; Gao, L.; Yang, J.; Chhowalla, M.; Gharahcheshmeh, M. H.; Gleason, K. K.; Choi, Y. S.; Hong, B. H.; Liu, Z. *Nat. Rev. Methods Primers* **2021**, *1*, 5.

(26) Khlyustova, A.; Cheng, Y.; Yang, R. *J. Mater. Chem. B* **2020**, *8*, 6588.
(27) Gleason, K. *Nat. Rev. Phys.* **2020**, *2*, 374.
(28) Gleason, K. K. *Nat. Rev. Phys.* **2020**, *2*, 347.
(29) Welchert, N. A.; Cheng, C.; Karandikar, P.; Gupta, M. *J. Vac. Sci. Technol., A* **2020**, *38*, 063405.
(30) Unger, K.; Coclite, A. *Pharmaceutics* **2020**, *12*, 904.
(31) Chen, Z.; Lau, K. K. S. *Macromolecules* **2019**, *52*, 5183.
(32) Mao, X.; Liu, A.; Tian, W.; Wang, X.; Gleason, K. K.; Hatton, T. A. *Adv. Funct. Mater.* **2018**, *28*, 1706028.
(33) Gleason, K. K. *Front. Bioeng. Biotechnol.* **2021**, *9*, 632753.
(34) Loyer, F.; Combrisson, A.; Omer, K.; Moreno-Couranjou, M.; Choquet, P.; Boscher, N. D. *ACS Appl. Mater. Interfaces* **2019**, *11*, 1335.
(35) Dorval Dion, C. A.; Tavares, J. R. *Powder Technol.* **2013**, *239*, 484.
(36) Lu, M.; Shao, D.; Wang, P.; Chen, D.; Zhang, Y.; Li, M.; Zhao, J.; Zhou, Y. *RSC Adv.* **2016**, *6*, 82688.
(37) Schröder, S.; Polonskyi, O.; Strunskus, T.; Faupel, F. *Mater. Today* **2020**, *37*, 35.
(38) Ozaydin-Ince, G.; Coclite, A. M.; Gleason, K. K. *Rep. Prog. Phys.* **2012**, *75*, 016501.
(39) Servi, A. T.; Kharraz, J.; Klee, D.; Notarangelo, K.; Eyob, B.; Guillen-Burrieza, E.; Liu, A.; Arafat, H. A.; Gleason, K. K. *J. Membr. Sci.* **2016**, *520*, 850.
(40) Olceroglu, E.; Hsieh, C. Y.; Rahman, M. M.; Lau, K. K.; McCarthy, M. *Langmuir* **2014**, *30*, 7556.
(41) Dianat, G.; Movsesian, N.; Gupta, M. *Macromolecules* **2018**, *51*, 10297.
(42) Schwartz, D.; Nguyen, T.; Chen, Z.; Lau, K. K. S.; Grady, M. C.; Shokoufandeh, A.; Soroush, M. *AIChE J.* **2022**, *68*, e17674.
(43) Chen, Y.; Ye, Y.; Chen, Z.-R. *J. Mater. Sci.* **2018**, *54*, 5907.
(44) Wei, X.; Bradley, L. C. *Langmuir* **2022**, *38*, 11550.
(45) Trujillo, N. J.; Baxamusa, S. H.; Gleason, K. K. *Chem. Mater.* **2009**, *21*, 742.
(46) Seidel, S.; Kwong, P.; Gupta, M. *Macromolecules* **2013**, *46*, 2976.
(47) Seidel, S.; Gupta, M. *J. Vac. Sci. Technol., A* **2014**, *32*, 041514.
(48) Bacheller, S.; Dianat, G.; Gupta, M. *ACS Appl. Polym. Mater.* **2021**, *3*, 6366.
(49) Welchert, N. A.; Nguyen, B.; Tsotsis, T. T.; Gupta, M. *Langmuir* **2021**, *37*, 13859.
(50) Kim, H.; Song, Y.; Park, S.; Kim, Y.; Mun, H.; Kim, J.; Kim, S.; Lee, K. G.; Im, S. G. *Adv. Funct. Mater.* **2022**, *32*, 2113253.
(51) Dianat, G.; Gao, K.; Prevoir, S.; Gupta, M. *ACS Appl. Polym. Mater.* **2020**, *2*, 3339.
(52) Su, P.; Liu, W.; Hong, Y.; Ye, Y.; Huang, S. *Mater. Today Chem.* **2022**, *24*, 100786.
(53) Armagan, E.; Ozaydin Ince, G. *Soft. Matter* **2015**, *11*, 8069.
(54) Karandikar, P.; Gupta, M. *Langmuir* **2017**, *33*, 7701.
(55) Oh, M. S.; Song, Y. S.; Kim, C.; Kim, J.; You, J. B.; Kim, T. S.; Lee, C. S.; Im, S. G. *ACS Appl. Mater. Interfaces* **2016**, *8*, 8782.
(56) Mehrabani, S.; Kwong, P.; Gupta, M.; Armani, A. M. *Appl. Phys. Lett.* **2013**, *102*, 241101.
(57) Song, Q.; Zhao, R.; Liu, T.; Gao, L.; Su, C.; Ye, Y.; Chan, S. Y.; Liu, X.; Wang, K.; Li, P.; Huang, W. *Chem. Eng. J.* **2021**, *418*, 129368.
(58) Matin, A.; Shafi, H.; Wang, M.; Khan, Z.; Gleason, K.; Rahman, F. *Desalination* **2016**, *379*, 108.
(59) Yang, R.; Xu, J.; Ozaydin-Ince, G.; Wong, S. Y.; Gleason, K. K. *Chem. Mater.* **2011**, *23*, 1263.
(60) Wang, H.; Shi, X.; Gao, A.; Lin, H.; Chen, Y.; Ye, Y.; He, J.; Liu, F.; Deng, G. *Appl. Surf. Sci.* **2018**, *433*, 869.
(61) Reichstein, W.; Sommer, L.; Veziroglu, S.; Sayin, S.; Schroder, S.; Mishra, Y. K.; Saygili, E. I.; Karayürek, F.; Açil, Y.; Wiltfang, J.; Gülses, A.; Faupel, F.; Cenk Aktas, O. *Polymers (Basel)* **2021**, *13*, 186.
(62) Zhi, B.; Song, Q.; Mao, Y. *RSC Adv.* **2018**, *8*, 4779.
(63) Christian, P.; Tumphart, S.; Ehmann, H. M. A.; Riegler, H.; Coclite, A. M.; Werzer, O. *Sci. Rep.* **2018**, *8*, 7134.
(64) Ghasemi-Mobarakeh, L.; Werzer, O.; Keimel, R.; Kolahreez, D.; Hadley, P.; Coclite, A. M. *J. Appl. Polym. Sci.* **2019**, *136*, 47858.
(65) Lee, B.; Jiao, A.; Yu, S.; You, J. B.; Kim, D. H.; Im, S. G. *Acta. Biomater.* **2013**, *9*, 7691.
(66) Shi, X.; Ye, Y.; Wang, H.; Liu, F.; Wang, Z. *ACS Appl. Mater. Interfaces* **2018**, *10*, 38449.
(67) Tufani, A.; Ozaydin Ince, G. *J. Membr. Sci.* **2017**, *537*, 255.
(68) Tufani, A.; Ozaydin Ince, G. *J. Membr. Sci.* **2019**, *575*, 126.
(69) Kim, M. J.; Pak, K.; Hwang, W. S.; Im, S. G.; Cho, B. J. *ACS Appl. Mater. Interfaces* **2018**, *10*, 37326.
(70) Mohammadmoradi, O.; Çelik, U.; Misirlioglu, I. B.; Ozaydin Ince, G. *Nanotechnology* **2021**, *32*, 435601.
(71) McMahon, B. J.; Pfluger, C. A.; Sun, B.; Ziemer, K. S.; Burkey, D. D.; Carrier, R. L. *J. Biomed. Mater. Res. Part A* **2014**, *102*, 2375.
(72) Fan, R.; Andrew, T. L. *J. Electrochem. Soc.* **2021**, *168*, 077518.
(73) Franz, G. *Processes* **2021**, *9*, 980.
(74) Getnet, T. G.; da Silva, G. F.; Duarte, I. S.; Kayama, M. E.; Rangel, E. C.; Cruz, N. C. *Materials (Basel)* **2020**, *13*, 3166.
(75) Abessolo Ondo, D.; Loyer, F.; Boscher, N. D. *Plasma Processes Polym.* **2021**, *18*, 2000222.
(76) Tenhaeff, W.; Gleason, K. *Adv. Funct. Mater.* **2008**, *18*, 979.
(77) Castro-Carranza, A.; Nolasco, J.; Bley, S.; Rückmann, M.; Meierhofer, F.; Mädler, L.; Voss, T.; Gutowski, J. *J. Polym. Sci., Part B: Polym. Phys.* **2016**, *54*, 1537.
(78) Oh, W. K.; Kim, S.; Shin, K. H.; Jang, Y.; Choi, M.; Jang, J. *Talanta* **2013**, *105*, 333.
(79) Cho, J.; Shin, K.-H.; Jang, J. *Thin Solid Films* **2010**, *518*, 5066.
(80) Peřinka, N.; Držková, M.; Randjelović, D. V.; Bondavalli, P.; Hajná, M.; Bober, P.; Syrový, T.; Bonnassieaux, Y.; Stejskal, J. *Key Eng. Mater.* **2015**, *644*, 61.
(81) Li, X.; Rafie, A.; Kalra, V.; Lau, K. K. S. *Langmuir* **2020**, *36*, 13079.
(82) Kim, Y. K.; Shin, K.-Y. *Appl. Surf. Sci.* **2021**, *547*, 149141.
(83) Back, J.-W.; Lee, S.; Hwang, C.-R.; Chi, C.-S.; Kim, J.-Y. *Macromol. Res.* **2011**, *19*, 33.
(84) Jang, J.; Li, X. L.; Oh, J. H. *Chem. Commun.* **2004**, 794.
(85) Xu, G.-L.; Liu, Q.; Lau, K. K. S.; Liu, Y.; Liu, X.; Gao, H.; Zhou, X.; Zhuang, M.; Ren, Y.; Li, J.; Shao, M.; Ouyang, M.; Pan, F.; Chen, Z.; Amine, K.; Chen, G. *Nat. Energy* **2019**, *4*, 484.
(86) Tian, L.; Yin, Y.; Zhao, J.; Jin, H.; Shang, Y.; Yan, S.; Dong, S. *Mater. Lett.* **2021**, *285*, 129141.
(87) Cetinkaya, M.; Boduroglu, S.; Demirel, M. C. *Polymer* **2007**, *48*, 4130.
(88) Demirel, M. C.; Boduroglu, S.; Cetinkaya, M.; Lakhtakia, A. *Langmuir* **2007**, *23*, 5861.
(89) Wei, L.; Lakhtakia, A. *Mater. Res. Innovations* **2013**, *17*, 129.
(90) Chen, H. Y.; Rouillard, J. M.; Gulari, E.; Lahann, J. *Proc. Natl. Acad. Sci. U.S.A.* **2007**, *104*, 11173.
(91) Moss, T.; Paulus, I. E.; Raps, D.; Altstädt, V.; Greiner, A. *e-Polymers* **2017**, *17*, 255.
(92) Chiu, Y.-R.; Hsu, Y.-T.; Wu, C.-Y.; Lin, T.-H.; Yang, Y.-Z.; Chen, H.-Y. *Chem. Mater.* **2020**, *32*, 1120.
(93) Hu, S.-M.; Lee, C.-Y.; Chang, Y.-M.; Xiao, J.-Q.; Kusanagi, T.; Wu, T.-Y.; Chang, N.-Y.; Christy, J.; Chiu, Y.-R.; Huang, C.-W.; Yang, Y.-C.; Chiang, Y.-C.; Chen, H.-Y., *Coatings* **2021**, *11*, 466.

(94) Lee, C. Y.; Hu, S. M.; Xiao, J. Q.; Chang, Y. M.; Kusanagi, T.; Wu, T. Y.; Chiu, Y. R.; Yang, Y. C.; Huang, C. W.; Chen, H. Y. *Polymers (Basel)* **2021**, *13*, 2073.
(95) Wei, L.; Vogler, E. A.; Ritty, T. M.; Lakhtakia, A. *Mater. Sci. Eng., C* **2011**, *31*, 1861.
(96) Bäte, M.; Neuber, C.; Giesa, R.; Schmidt, H.-W. *Macromol. Rapid Commun.* **2004**, *25*, 371.
(97) Neuber, C.; Bäte, M.; Giesa, R.; Schmidt, H.-W. *J. Mater. Chem.* **2006**, *16*, 3466.
(98) Chang, Y.-M.; Xiao, J.-Q.; Christy, J.; Wu, C.-Y.; Huang, C.-W.; Wu, T.-Y.; Chiang, Y.-C.; Lin, T.-H.; Chen, H.-Y. *Mater. Today Bio.* **2022**, *16*, 100403.
(99) Wu, T.-Y.; Lin, T.-H.; Chen, H.-Y. *Mater. Today Adv.* **2022**, *16*, 100292.
(100) Wu, T. Y.; Wu, C. Y.; Christy, J.; Chiang, Y. C.; Guan, Z. Y.; Yu, J.; Chen, H. Y. *Adv. Mater. Interfaces* **2021**, *8*, 2100929.
(101) Chiang, Y. C.; Yeh, H. W.; Hu, S. M.; Wu, C. Y.; Wu, T. Y.; Chen, C. H.; Liao, P. C.; Guan, Z. Y.; Cheng, N. C.; Chen, H. Y. *Mater. Today Bio.* **2022**, *13*, 100213.
(102) Wu, C. Y.; Guo, C. L.; Yang, Y. C.; Huang, C. W.; Zeng, J. Y.; Guan, Z. Y.; Chiang, Y. C.; Wang, P. Y.; Chen, H. Y. *ACS Appl. Bio Mater.* **2020**, *3*, 7193.
(103) Bognitzki, M.; Hou, H.; Ishaque, M.; Frese, T.; Hellwig, M.; Schwarte, C.; Schaper, A.; Wendorff, J. H.; Greiner, A. *Adv. Mater.* **2000**, *12*, 637.
(104) Tung, H. Y.; Guan, Z. Y.; Liu, T. Y.; Chen, H. Y. *Nat. Commun.* **2018**, *9*, 2564.
(105) Liu, Y.-C.; Jhang, J.-W.; Liu, K.; Pan, H.; Chen, H.-Y.; Wang, P.-Y. *Coatings* **2022**, *12*, 311.
(106) Sim, J. H.; Chae, H.; Kim, S.-B.; Yoo, S. *Sci. Rep.* **2022**, *12*, 9506.
(107) Coclite, A. M.; Gleason, K. K. *J. Appl. Phys.* **2012**, *111*, 073516.
(108) Shao, J.; Sheng, W.; Wang, C.; Ye, Y. *Chem. Eng. J.* **2021**, *416*, 128043.
(109) Luo, Z.; Lu, Y.; Singer, D. W.; Berck, M. E.; Somers, L. A.; Goldsmith, B. R.; Johnson, A. T. C. *Chem. Mater.* **2011**, *23*, 1441.
(110) Gharahcheshmeh, M. H.; Tavakoli, M.; Gleason, E. F.; Robinson, M. T.; Kong, J.; Gleason, K. *Sci. Adv.* **2019**, *5*, saay0414.
(111) Drewelow, G.; Wook Song, H.; Jiang, Z.-T.; Lee, S. *Appl. Surf. Sci.* **2020**, *501*, 144105.
(112) Wang, X.; Zhang, X.; Sun, L.; Lee, D.; Lee, S.; Wang, M.; Zhao, J.; Shao-Horn, Y.; Dincă, M.; Palacios, T.; Gleason, K. K. *Sci. Adv.* **2018**, *4*, eaat5780.
(113) Kaviani, S.; Mohammadi Ghaleni, M.; Tavakoli, E.; Nejati, S. *ACS Appl. Polym. Mater.* **2019**, *1*, 552.
(114) Chen, H.-Y.; Lahann, J. *Langmuir* **2011**, *27*, 34.
(115) Ortigoza-Diaz, J.; Scholten, K.; Larson, C.; Cobo, A.; Hudson, T.; Yoo, J.; Baldwin, A.; Weltman Hirschberg, A.; Meng, E. *Micromachines* **2018**, *9*, 422.
(116) Bally-Le Gall, F.; Friedmann, C.; Heinke, L.; Arslan, H.; Azucena, C.; Welle, A.; Ross, A. M.; Wöll, C.; Lahann, J. *ACS Nano* **2015**, *9*, 1400.
(117) Hsu, Y.-T.; Wu, C.-Y.; Guan, Z.-Y.; Sun, H.-Y.; Mei, C.; Chen, W.-C.; Cheng, N.-C.; Yu, J.; Chen, H.-Y. *Sci. Rep.* **2019**, *9*, 7644.
(118) Montero, L.; Baxamusa, S. H.; Borros, S.; Gleason, K. K. *Chem. Mater.* **2009**, *21*, 399.
(119) Chen, Y.-F.; Khlyustova, A.; Yang, R. *J. Vac. Sci. Technol., A* **2022**, *40*, 033406.
(120) Kim, M. J.; Jeong, J.; Lee, T. I.; Kim, J.; Tak, Y.; Park, H.; Im, S. G.; Cho, B. J. *Macromol. Mater. Eng.* **2021**, *306*, 2000608.
(121) Schamberger, F.; Ziegler, A.; Franz, G. *J. Vac. Sci. Technol., B* **2012**, *30*, 051801.
(122) Chen, L.; Xu, H.; Li, T.; Zhang, M.; Han, X.; Jin, Y.; Wang, W. *J. Micromech. Microeng.* **2022**, *32*, 044005.
(123) Gołda, M.; Brzychczy-Włoch, M.; Faryna, M.; Engvall, K.; Kotarba, A. *Mater. Sci. Eng., C* **2013**, *33*, 4221.
(124) Brancato, L.; Decrop, D.; Lammertyn, J.; Puers, R. *Materials (Basel)* **2018**, *11*, 1109.
(125) Hsu, J. M.; Rieth, L.; Kammer, S.; Orthner, M.; Solzbacher, F. *Sens. Mater.* **2008**, *20*, 87.
(126) Truong, T. L.; Luong, N. D.; Nam, J.-D.; Lee, Y.; Choi, H. R.; Koo, J. C.; Nguyen, H. N. *Macromol. Res.* **2007**, *15*, 465.
(127) Goktas, H.; Wang, X.; Ugur, A.; Gleason, K. K. *Macromol. Rapid Commun.* **2015**, *36*, 1283.
(128) Amirzada, M. R.; Tatzel, A.; Viereck, V.; Hillmer, H. *Appl. Nanosci.* **2016**, *6*, 215.
(129) Nie, S.; Li, Z.; Yao, Y.; Jin, Y. *Front. Chem.* **2021**, *9*, doi: 10.3389/fchem.2021.803509.
(130) Moni, P.; Lau, J.; Mohr, A. C.; Lin, T. C.; Tolbert, S. H.; Dunn, B.; Gleason, K. K. *ACS Appl. Energy Mater.* **2018**, *1*, 7093.
(131) Zhao, J.; Wang, M.; Gleason, K. K. *Adv. Mater. Interfaces* **2017**, *4*, 1700270.
(132) Lee, H. S.; Kim, H.; Lee, J. H.; Kwak, J. B. *Coatings* **2019**, *9*, 430.
(133) Jeong, K.; Kwak, M. J.; Kim, Y.; Lee, Y.; Mun, H.; Kim, M. J.; Cho, B. J.; Choi, S. Q.; Im, S. G. *Soft. Matter* **2022**, *18*, 6907.
(134) Smith, P. M.; Su, L.; Gong, W.; Nakamura, N.; Reeja-Jayan, B.; Shen, S. *RSC Adv.* **2018**, *8*, 19348.
(135) Deng, X.; Lahann, J. *J. Appl. Polym. Sci.* **2014**, *131*, 40315.
(136) Sun, H.-Y.; Fang, C.-Y.; Lin, T.-J.; Chen, Y.-C.; Lin, C.-Y.; Ho, H.-Y.; Chen, M. H.-C.; Yu, J.; Lee, D.-J.; Chang, C.-H.; Chen, H.-Y. *Adv. Mater. Interfaces* **2014**, *1*, 1400093.
(137) Chen, P. J.; Chen, H. Y.; Tsai, W. B. *Polymers (Basel)* **2022**, *14*, 225.
(138) Im, S. G.; Kim, B.-S.; Lee, L. H.; Tenhaeff, W. E.; Hammond, P. T.; Gleason, K. K. *Macromol. Rapid Commun.* **2008**, *29*, 1648.
(139) Jiang, X.; Chen, H.-Y.; Galvan, G.; Yoshida, M.; Lahann, J. *Adv. Funct. Mater.* **2008**, *18*, 27.
(140) Alf, M. E.; Asatekin, A.; Barr, M. C.; Baxamusa, S. H.; Chelawat, H.; Ozaydin-Ince, G.; Petruczok, C. D.; Sreenivasan, R.; Tenhaeff, W. E.; Trujillo, N. J.; Vaddiraju, S.; Xu, J.; Gleason, K. K. *Adv. Mater.* **2010**, *22*, 1993.
(141) Li, W.; Bradley, L. C.; Watkins, J. J. *ACS Appl. Mater. Interfaces* **2019**, *11*, 5668.
(142) Chiang, Y. C.; Ho, C. P.; Wang, Y. L.; Chen, P. C.; Wang, P. Y.; Chen, H. Y. *Polymers (Basel)* **2019**, *11*, 1595.
(143) Tung, H.-Y.; Sun, T.-P.; Sun, H.-Y.; Guan, Z.-Y.; Hu, S.-K.; Chao, L.; Chen, H.-Y. *Appl. Mater. Today* **2017**, *7*, 77.
(144) De Luna, M. M.; Karandikar, P.; Gupta, M. *ACS Appl. Nano Mater.* **2018**, *1*, 6575.
(145) Vaddiraju, S.; Gleason, K. K. *Nanotechnology* **2010**, *21*, 125503.
(146) Soto, D.; Ugur, A.; Farnham, T. A.; Gleason, K. K.; Varanasi, K. K. *Adv. Funct. Mater.* **2018**, *28*, 1707355.
(147) Xu, J.; Gleason, K. K. *Chem. Mater.* **2010**, *22*, 1732.
(148) Xu, J.; Zhang, Y.; Yu, Q.; Zhang, L. *Thin-Walled Struct.* **2022**, *170*, 108619.
(149) Inamuddin, D.; Mohammad, A.; Asiri, A. M. *Organic-Inorganic Composite Polymer Electrolyte Membranes*; Springer: Cham, **2017**.
(150) Tenhaeff, W. E.; Gleason, K. K. *Adv. Funct. Mater.* **2008**, *18*, 979.
(151) Gupta, M.; Kapur, V.; Pinkerton, N. M.; Gleason, K. K. *Chem. Mater.* **2008**, *20*, 1646.
(152) Nedaei, M.; Motezakker, A. R.; Zeybek, M. C.; Sezen, M.; Ince, G. O.; Kosar, A. *Exp. Therm. Fluid Sci.* **2017**, *86*, 130.
(153) Chen, H. Y.; Elkasabi, Y.; Lahann, J. *J. Am. Chem. Soc.* **2006**, *128*, 374.

(154) Jang, J.; Lim, B. *Angew. Chem. Int. Ed. Engl.* **2003**, *42*, 5600.
(155) Malkov, G. S.; Fisher, E. R. *Plasma Processes Polym.* **2010**, *7*, 695.
(156) Sun, H.; Fu, C.; Gao, Y.; Guo, P.; Wang, C.; Yang, W.; Wang, Q.; Zhang, C.; Wang, J.; Xu, J. *Nanotechnology* **2018**, *29*, 305601.
(157) Jeong, G.; Oh, J.; Jang, J. *Biosens. Bioelectron.* **2019**, *131*, 30.
(158) Mansurnezhad, R.; Ghasemi-Mobarakeh, L.; Coclite, A. M.; Beigi, M. H.; Gharibi, H.; Werzer, O.; Khodadadi-Khorzoughi, M.; Nasr-Esfahani, M. H. *Mater. Sci. Eng., C.* **2020**, *110*, 110623.
(159) Beauregard, N.; Al-Furaiji, M.; Dias, G.; Worthington, M.; Suresh, A.; Srivastava, R.; Burkey, D. D.; McCutcheon, J. R. *Polymers (Basel)* **2020**, *12*, 2074.
(160) Vilaro, I.; Yague, J. L.; Borros, S. *ACS Appl. Mater. Interfaces* **2017**, *9*, 1057.
(161) Dianat, G.; Seidel, S.; De Luna, M. M.; Gupta, M. *Macromol. Mater. Eng.* **2016**, *301*, 1037.
(162) Demirel, M. C. *Colloids Surf., A* **2008**, *321*, 121.
(163) Huang, X.; Sun, M.; Shi, X.; Shao, J.; Jin, M.; Liu, W.; Zhang, R.; Huang, S.; Ye, Y. *Chem. Eng. J.* **2023**, *454*, 139981.
(164) Enright, R. N.; Bradley, L. C. *Adv. Funct. Mater.* **2022**, *32*, 2204887.
(165) Chen, H. Y.; Lahann, J. *Adv. Mater.* **2007**, *19*, 3801.
(166) Deng, X.; Friedmann, C.; Lahann, J. *Angew. Chem. Int. Ed. Engl.* **2011**, *50*, 6522.
(167) Bally-Le Gall, F.; Hussal, C.; Kramer, J.; Cheng, K.; Kumar, R.; Eyster, T.; Baek, A.; Trouillet, V.; Nieger, M.; Bräse, S.; Lahann, J. *Chem. – Eur. J.* **2017**, *23*, 13342.
(168) Bally, F.; Cheng, K.; Nandivada, H.; Deng, X.; Ross, A. M.; Panades, A.; Lahann, J. *ACS Appl. Mater. Interfaces* **2013**, *5*, 9262.
(169) Ross, A.; Durmaz, H.; Cheng, K.; Deng, X.; Liu, Y.; Oh, J.; Chen, Z.; Lahann, J. *Langmuir* **2015**, *31*, 5123.
(170) Jiang, X.; Chen, H. Y.; Galvan, G.; Yoshida, M.; Lahann, J. *Adv. Funct. Mater.* **2008**, *18*, 27.
(171) Suh, K. Y.; Langer, R.; Lahann, J. *Appl. Phys. Lett.* **2003**, *83*, 4250.
(172) Andou, Y.; Nishida, H.; Endo, T. *Chem. Commun.* **2006**, *48*, 5018.
(173) Gomi, S.; Andou, Y.; Nishida, H. *J. Photopolym. Sci. Technol.* **2016**, *29*, 17.
(174) Jang, J.; Lim, B.; Choi, M. *Chem. Commun.* **2005**, 4214.
(175) Ohsawa, Y.; Takahashi, R.; Maruyama, S.; Matsumoto, Y. *ACS Macro Lett.* **2016**, *5*, 1009.
(176) Takahashi, R.; Maruyama, S.; Ohsawa, Y.; Matsumoto, Y. *Chem. Lett.* **2018**, *47*, 1460.
(177) Watanabe, H.; Takazawa, R.; Takahashi, R.; Maruyama, S.; Matsumoto, Y. *ACS Appl. Nano Mater.* **2020**, *3*, 9610.
(178) Tao, R.; Anthamatten, M. *Macromol. Rapid Commun.* **2013**, *34*, 1755.
(179) Tao, R.; Anthamatten, M. *Macromol. Mater. Eng.* **2015**, *301*, 99.
(180) Huo, N.; Ye, S.; Ouderkirk, A. J.; Tenhaeff, W. E. *ACS Appl. Polym. Mater.* **2022**, *4*, 7300.
(181) Elkasabi, Y. M.; Lahann, J.; Krebsbach, P. H. *Biomaterials* **2011**, *32*, 1809.
(182) Elkasabi, Y.; Ross, A. M.; Oh, J.; Hoepfner, M. P.; Fogler, H. S.; Lahann, J.; Krebsbach, P. H. *Chem. Vap. Deposition* **2014**, *20*, 23.
(183) Ozaydin-Ince, G.; Gleason, K. K.; Demirel, M. C. *Soft Matter* **2011**, *7*, 638.
(184) Wu, C.-Y.; Kuo, P.-H.; Duh, J.-G. *Surf. Coat. Technol.* **2021**, *421*, 127418.
(185) Balkan, A.; Armagan, E.; Ozaydin Ince, G. *Beilstein J. Nanotechnol.* **2017**, *8*, 872.
(186) Ozaydin Ince, G.; Demirel, G.; Gleason, K. K.; Demirel, M. C. *Soft Matter* **2010**, *6*, 1635.
(187) Ince, G. O.; Armagan, E.; Erdogan, H.; Buyukserin, F.; Uzun, L.; Demirel, G. *ACS Appl. Mater. Interfaces* **2013**, *5*, 6447.
(188) Franklin, T.; Streever, D. L.; Yang, R. *Chem. Mater.* **2022**, *34*, 5960.
(189) Su, C.; Hu, Y.; Song, Q.; Ye, Y.; Gao, L.; Li, P.; Ye, T. *ACS Appl. Mater. Interfaces* **2020**, *12*, 18978.
(190) Su, C.; Ye, Y.; Qiu, H.; Zhu, Y. *ACS Appl. Mater. Interfaces* **2021**, *13*, 10553.
(191) Liu, Z.; Jiang, X.; Li, Z.; Zheng, Y.; Nie, J.-J.; Cui, Z.; Liang, Y.; Zhu, S.; Chen, D.; Wu, S. *Chem. Eng. J.* **2022**, *437*, 135401.
(192) Cihanoğlu, G.; Ebil, Ö. *J. Mater. Sci.* **2021**, *56*, 11970.
(193) Guo, L.; Li, J.; Zhang, X.; Guo, S. *Prog. Org. Coat.* **2022**, *172*, 107099.
(194) Xia, T.; Liu, W.; Ye, Y. *J. Mater. Sci.* **2022**, *57*, 8314.
(195) Perrotta, A.; Werzer, O.; Coclite, A. M. *Adv. Eng. Mater.* **2018**, *20*, 1700639.
(196) Cong, S.; Liu, X.; Guo, F. *Int. J. Heat Mass Transfer* **2019**, *129*, 764.
(197) Tufani, A.; Ozaydin Ince, G. *J. Appl. Polym. Sci.* **2015**, *132*, 42453.
(198) Wu, J.-T.; Wu, C.-Y.; Fan, S.-K.; Hsieh, C.-C.; Hou, Y.-C.; Chen, H.-Y. *Chem. Mater.* **2015**, *27*, 7028.
(199) Jung, I. Y.; You, J. B.; Choi, B. R.; Kim, J. S.; Lee, H. K.; Jang, B.; Jeong, H. S.; Lee, K.; Im, S. G.; Lee, H. *Adv. Healthcare Mater.* **2016**, *5*, 2168.
(200) Kim, M. J.; Lee, C.; Jeong, J.; Kim, S.; Lee, T. I.; Shin, E. J.; Hwang, W. S.; Im, S. G.; Cho, B. J. *Adv. Electron. Mater.* **2021**, *7*, 2001197
(201) Jeong, J.; Kim, M. J.; Hwang, W. S.; Cho, B. J. *Adv. Electron. Mater.* **2021**, *7*, 2100375.
(202) Khalil, K.; Soto, D.; Farnham, T.; Paxson, A.; Katmis, A. U.; Gleason, K.; Varanasi, K. K. *Joule* **2019**, *3*, 1377.
(203) Nejati, S.; Lau, K. K. *Nano Lett.* **2011**, *11*, 419.
(204) Sreenivasan, R.; Bassett, E. K.; Hoganson, D. M.; Vacanti, J. P.; Gleason, K. K. *Biomaterials* **2011**, *32*, 3883.